SANDIA REPORT

SAND2010-6119
Unlimited Release
Printed September 2010

The Application of Quaternions and Other Spatial Representations to the Reconstruction of Re-entry Vehicle Motion

Vincent De Sapio

Prepared by
Sandia National Laboratories
Albuquerque, New Mexico 87185 and Livermore, California 94550

Sandia National Laboratories is a multi-program laboratory managed and operated by Sandia Corporation, a wholly owned subsidiary of Lockheed Martin Corporation, for the U.S. Department of Energy's National Nuclear Security Administration under contract DE-AC04-94AL85000.

Issued by Sandia National Laboratories, operated for the United States Department of Energy by Sandia Corporation.

Available to DOE and DOE contractors from
U.S. Department of Energy
Office of Scientific and Technical Information
P.O. Box 62
Oak Ridge, TN 37831

Telephone: (865) 576-8401
Facsimile: (865) 576-5728
E-Mail: reports@adonis.osti.gov
Online ordering: http://www.osti.gov/bridge

Available to the public from
U.S. Department of Commerce
National Technical Information Service
5285 Port Royal Rd
Springfield, VA 22161

Telephone: (800) 553-6847
Facsimile: (703) 605-6900
E-Mail: orders@ntis.fedworld.gov
Online ordering: http://www.ntis.gov/help/ordermethods.asp?loc=7-4-0#online

SAND2010-6119
Unlimited Release
Printed September 2010

The Application of Quaternions and Other Spatial Representations to the Reconstruction of Re-entry Vehicle Motion

Vincent De Sapio
Sandia National Laboratories
MS 9159
P.O. Box 969, Livermore, CA 94551 U.S.A.
vdesap@sandia.gov

Abstract

The analysis of spacecraft kinematics and dynamics requires an efficient scheme for spatial representation. While the representation of displacement in three dimensional Euclidean space is straightforward, orientation in three dimensions poses particular challenges. The unit quaternion provides an approach that mitigates many of the problems intrinsic in other representation approaches, including the ill-conditioning that arises from computing many successive rotations. This report focusses on the computational utility of unit quaternions and their application to the reconstruction of re-entry vehicle (RV) motion history from sensor data. To this end they will be used in conjunction with other kinematic and data processing techniques.

We will present a numerical implementation for the reconstruction of RV motion solely from gyroscope and accelerometer data. This will make use of unit quaternions due to their numerical efficacy in dealing with the composition of many incremental rotations over a time series. In addition to signal processing and data conditioning procedures, algorithms for numerical quaternion-based integration of gyroscope data will be addressed, as well as accelerometer triangulation and integration to yield RV trajectory. Actual processed flight data will be presented to demonstrate the implementation of these methods.

Contents

Appendix

Figures

Notation

General Mathematical Objects

Sets

The following standard set notation will be employed.

$\{\}$	designation of a set
$\mid$	such that
$\forall$	for all
$\in$	element of
$\mathbb{R}$	set of real numbers
$\mathbb{R}^n$	set of real n-dimensional vectors
$\mathbb{R}^{m\times n}$	set of real $m \times n$ matrices
$\mathbb{C}$	set of complex numbers
$\mathbb{H}$	set of quaternions

Scalars

Scalars (rank 0 tensors) will always be represented with non-bold italic characters (e.g. a). These include scalars as well as scalar components of vectors and matrices. Scalar components of vectors and matrices will be denoted with a subscripted index to the right of the scalar symbol (e.g. v_i, M_{ij}). The following standard operators will be employed.

δ	variation
$\frac{d\square}{d\square}$	derivative
$\dot{\square}$	time derivative

Complex Numbers and Quaternions

Complex numbers and quaternions will always be represented with non-bold lower case (typically) italic characters. The components can be shown as a sum of the real and imaginary parts. For example,

$$z = a + \mathbf{i}b \tag{1}$$

$$h = h_0 + h_1\mathbf{i} + h_2\mathbf{j} + h_3\mathbf{k} \tag{2}$$

Vectors, Points, and Line Segments

Vectors (rank 1 tensors) will always be represented with bold lower case (typically) characters. Unit vectors will be denoted with a $\hat{\square}$, as in $\hat{\mathbf{k}}$. The components of a vector can be shown as an array or as a linear combination of basis vectors. Basis vectors will be denoted as $\hat{\mathbf{e}}$. For example,

$$\mathbf{v} = \begin{pmatrix} v_1 \\ v_2 \\ v_3 \end{pmatrix} = v_1\hat{\mathbf{e}}_1 + v_2\hat{\mathbf{e}}_2 + v_3\hat{\mathbf{e}}_3 \tag{3}$$

Points will be represented using non-bold italic characters. Line segments between two points will be denoted with an $\overrightarrow{\square}$, as in $\overrightarrow{AB}$.

Matrices and Tensors

Matrices (rank 2 tensors) will always be represented with bold upper case (typically) characters. The components can be shown as an array or as a linear combination of dyads. Dyads consist of a pair of base vectors separated by an outer product symbol, $\otimes$. For example,

$$\mathbf{M} = \begin{pmatrix} M_{11} & M_{12} \\ M_{21} & M_{22} \end{pmatrix} = M_{11}\hat{\mathbf{e}}_1 \otimes \hat{\mathbf{e}}_1 + M_{12}\hat{\mathbf{e}}_1 \otimes \hat{\mathbf{e}}_2 + M_{21}\hat{\mathbf{e}}_2 \otimes \hat{\mathbf{e}}_1 + M_{22}\hat{\mathbf{e}}_2 \otimes \hat{\mathbf{e}}_2 \tag{4}$$

The identity matrix will be denoted as **1** and the *zero* matrix will be denoted as **0**.

Vector and Matrix Operators

The following standard vector and matrix operators will be employed.

$\cdot$	dot product
$\|\square\|$	norm
$\times$	cross product
$\otimes$	outer product
δ	variation
$\frac{d\square}{ds}$	derivative with respect to a scalar, s
$\dot{\square}$	time derivative

Kinematic Objects

Objects having a kinematic meaning inherit all of the aforementioned rules with respect to their mathematical type. Additionally they adhere to the following with regard to their physical type.

A position vector, **r**, will use a right subscript to denote the material point it refers to and a left superscript to denote the basis it is expressed in. Velocity, **v** and acceleration, **a**, vectors will additionally denote the

frame which motion is relative to using a ":" separator in the right subscript. Angular velocity, ω, and angular acceleration vectors, α, will use a right subscript to denote the body they refer to and a left superscript to denote the basis they are expressed in. As with velocity they will additionally denote the frame which motion is relative to using a ":". Any annotation can be omitted if the information conveyed by it is already clear from the context.

Coordinate transformation matrices, including both orthogonal rotation matrices, $\mathbf{Q}$, and homogenous transformation matrices, $\mathbf{T}$, will denote the frame of interest using a left subscript and the embedding frame using a left superscript. Unit quaternions, h, will use similar annotation. Again, any annotation can be omitted if the information conveyed by it is already clear from the context.

${}^{\mathcal{B}}\mathbf{r}_{G_{\mathcal{A}}}$	position vector of center of mass, G, of body $\mathcal{A}$ expressed in $\mathcal{B}$
${}^{\mathcal{B}}\mathbf{d}_{\vec{AB}}$	displacement vector between points A and B, expressed in $\mathcal{B}$
${}^{\mathcal{A}}_{\mathcal{B}}\mathbf{Q}$	rotation matrix of $\mathcal{B}$ with respect to $\mathcal{A}$
$\mathbf{Q}_k(\theta)$	rotation matrix representing a spin of θ about $\hat{\mathbf{k}}$
${}^{\mathcal{A}}_{\mathcal{B}}h$	quaternion of $\mathcal{B}$ with respect to $\mathcal{A}$
$h_k(\theta)$	quaternion representing a spin of θ about $\hat{\mathbf{k}}$
$\{\alpha,\beta,\gamma\}$	Euler angle set angles
${}^{\mathcal{A}}_{\mathcal{B}}\mathbf{T}$	homogenous transformation matrix of $\mathcal{B}$ with respect to $\mathcal{A}$
${}^{\mathcal{B}}\mathbf{v}_{G_{\mathcal{A}}:\mathcal{O}}$	velocity vector of center of mass, G, of body $\mathcal{A}$, relative to $\mathcal{O}$, expressed in $\mathcal{B}$
${}^{\mathcal{B}}\boldsymbol{\omega}_{\mathcal{A}:\mathcal{O}}$	angular velocity vector of body $\mathcal{A}$, relative to $\mathcal{O}$, expressed in $\mathcal{B}$
${}^{\mathcal{B}}\boldsymbol{\Omega}_{\mathcal{A}:\mathcal{O}}$	angular velocity tensor of body $\mathcal{A}$, relative to $\mathcal{O}$, expressed in $\mathcal{B}$
${}^{\mathcal{B}}\omega_{\mathcal{A}:\mathcal{O}}$	angular velocity quaternion of body $\mathcal{A}$, relative to $\mathcal{O}$, expressed in $\mathcal{B}$
${}^{\mathcal{B}}\mathbf{E}_{\mathcal{A}}$	Jacobian (with respect to angle set rates) of angular velocity of body $\mathcal{A}$ expressed in $\mathcal{B}$
${}^{\mathcal{B}}\mathbf{a}_{G_{\mathcal{A}}:\mathcal{O}}$	acceleration vector of center of mass, G, of body $\mathcal{A}$, relative to $\mathcal{O}$, expressed in $\mathcal{B}$
${}^{\mathcal{B}}\boldsymbol{\alpha}_{\mathcal{A}:\mathcal{O}}$	angular acceleration vector of body $\mathcal{A}$, relative to $\mathcal{O}$, expressed in $\mathcal{B}$

1 Introduction

A number of spatial representations have been useful in the analysis of spacecraft kinematics and dynamics [1] [8] [11]. While the representation of displacement in three dimensional Euclidean space is straightforward, orientation in three dimensions, the special orthogonal group $SO(3)$, poses particular challenges. Traditional representations of orientation include orthogonal matrices, angle-sets, and axis-angle parameters. Each of these are suitable for some purposes but problematic for others. For example, angle sets which represent orientation using a concise sequence of three rotations about successive coordinate axes (either fixed or relative) suffer from singularities [2]. The orthogonal matrix [5], $\mathbb{R}^{3\times3}$, which offers a straightforward algebra for generating composite rotations involves an excess of parameters (9 matrix components) to represent orientation. Additionally, it is ill-suited to certain computational applications that involve computing many successive rotations. This is due to the fact that successive multiplications of orthogonal matrices at finite precision results in matrices that lose their orthogonality properties.

The unit quaternion provides an approach that mitigates many of the problems intrinsic in other representation approaches. In the years subsequent to their introduction in the 19th century by William Rowan Hamilton [6] [7] [9], the use of quaternions was largely obviated by the vector techniques developed by Gibbs and others. In recent years there have been a number of new applications for quaternions, especially in computer graphics. In this area, they have demonstrated particular efficacy when used for interpolating between orientation states, yielding smooth rotational transitions. Their numerical efficiency and stability, make them especially amenable to general computational use. Due to their computational utility quaternions will be applied here as a an effective tool in reconstructing re-entry vehicle (RV) motion history from sensor data. They will be used in conjunction with other kinematic and data processing techniques to this end.

2 Overview of the RV Data Analysis Process

The RV data analysis process presented here involves a number of input data sets and a number of analysis processes. The input data consists of the following:

- Three (3) channels of gyroscope data
- Three (3) channels of accelerometer data
- Initial conditions for position and velocity
- Position and orientation of each of the accelerometers in the local RV reference frame
- CAD model of the RV

The major data analysis processes involve the following:

- Data conditioning of input data (smoothing, interpolation, fitting)
- Reformulating angular velocity as rate of change of a unit quaternion
- Numerical differentiation and integration
- Triangulating center of mass acceleration
- Data conditioning of numerically integrated data (high pass filtering)
- Exporting output data into a motion file
- Visualization

Data conditioning, including low pass filtering (smoothing), interpolation, and fitting is performed on the input gyroscope data. Next, the angular velocity data is reformulated as the rate of change of unit quaternions. Numerical differentiation of the smoothed angular velocity data and integration of the quaternion rate data is performed to yield a time history of the RV orientation. Next, the accelerometer data is triangulated to compute the acceleration of the center of mass of the RV. This is integrated and filtered (high pass) to yield the velocity and position of the center of mass. *Figure 1* depicts this process flow.

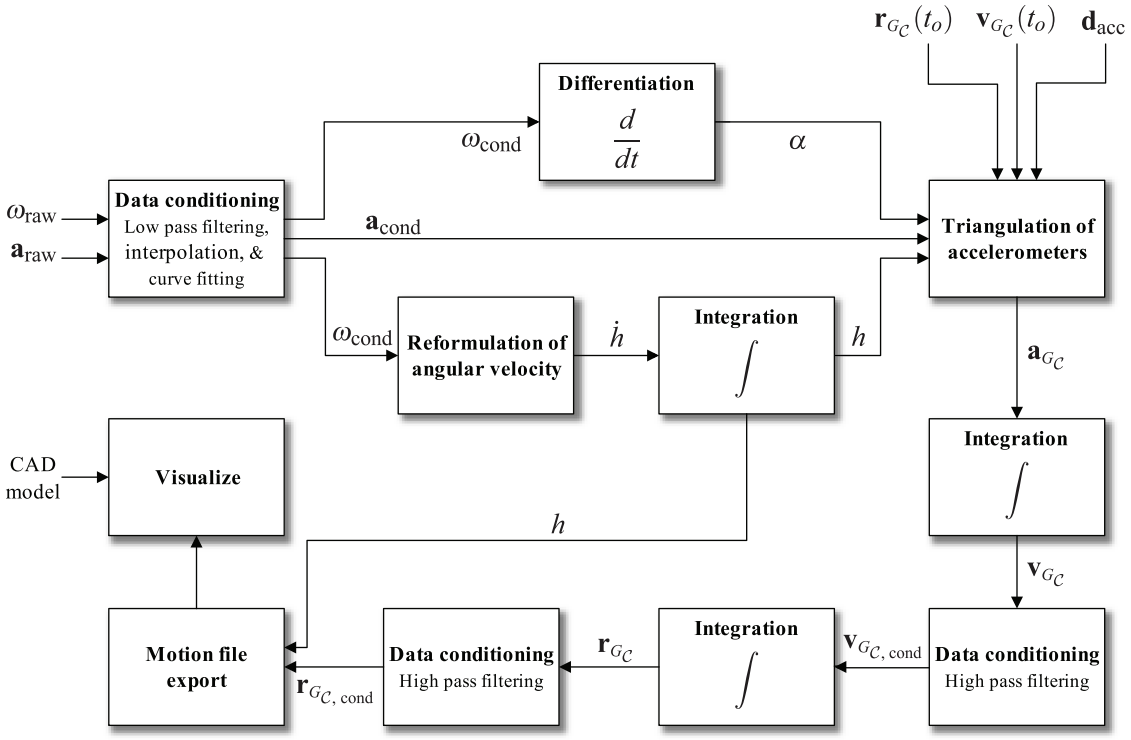

Figure 1. Process flow for the RV data analysis. Data conditioning is performed on the input gyroscope data. Angular velocity is reformulated using unit quaternions. Numerical differentiation of the angular velocity data and integration of the quaternion rate data is performed. The accelerometer data is used to compute the acceleration of the RV center of mass. This is integrated to yield velocity and position of the center of mass.

3 Data Conditioning

3.1 Low Pass Filtering (Smoothing)

Low pass filtering was primarily used for data smoothing. This is fundamentally important since data acquisition inherently involves the inclusion of noise. Since numerical derivatives need to be taken, clean data is especially crucial. The primary smoothing algorithm used was a Savitzky-Golay filter. A first order Savitzky-Golay filter (moving window averaging) was employed. *Figure 2* shows the results of this smoothing algorithm applied to the raw *y*-axis gyroscope data.

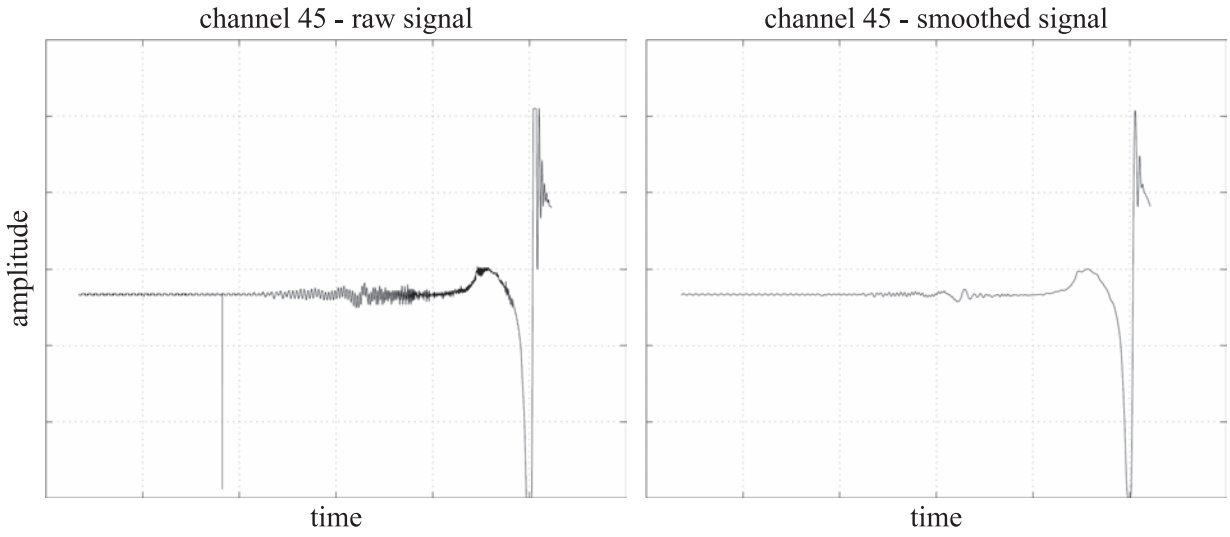

Figure 2. Results of smoothing channel 45 *y*-axis gyroscope data using a first order Savitzky-Golay filter. Units have been intentionally omitted. (Left) Raw signal. (Right) Smoothed signal.

3.2 Interpolation and Curve Fitting

Numerous linear interpolations were performed to synchronize the time series data reported from the various instruments. This facilitated all the data channels referring to a common time series. Additionally, curve fitting was performed to fill in a portion of data from a saturated accelerometer. A small portion of data from another RV flight was inserted into the saturated region. A third order (cubic) polynomial fit was performed to generate an expression for the data in the saturated region. *Figure 3* displays the results of this.

3.3 High Pass Filtering

High pass filtering was used to remove low frequency DC drift from numerically integrated signals. To this end digital Butterworth filters were designed to remove low frequency elements while preserving the higher

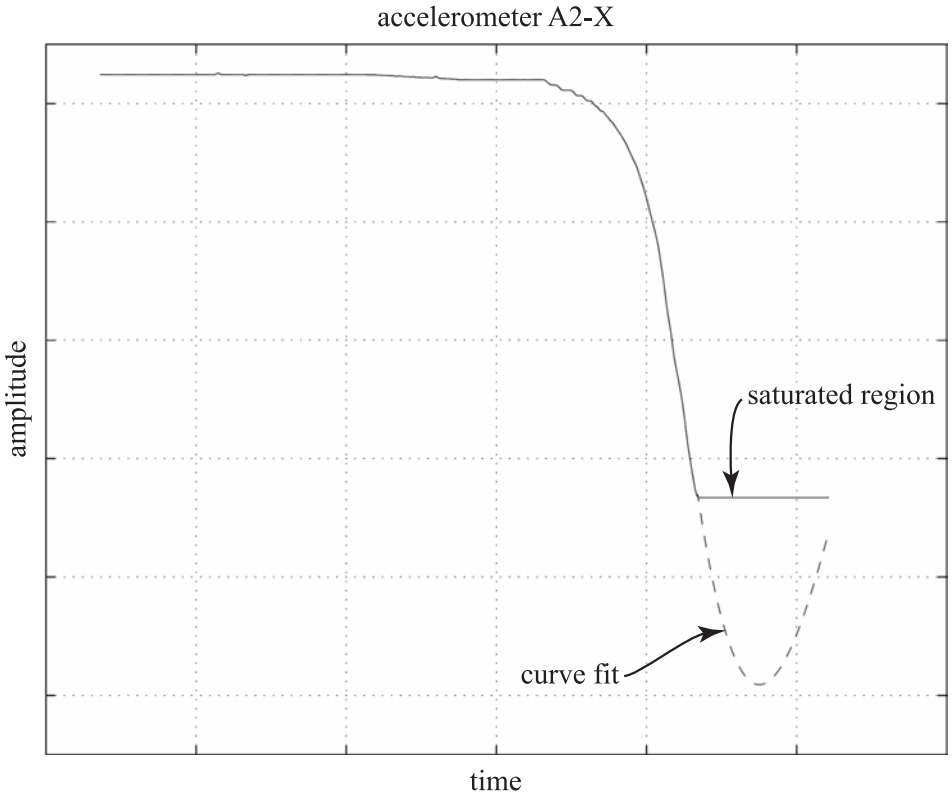

Figure 3. Curve fitting in saturated region of the accelerometer. A third order (cubic) polynomial fit was performed using data points from another RV flight that were inserted into the saturated region. Units have been intentionally omitted.

frequency elements of the signal. The digital transfer function [4] for performing this filtering is represented as,

$$H(z) = \frac{B(z)}{A(z)} = \frac{b_1 + b_2 z^{-1} + \cdots + b_{n+1} z^{-n}}{a_1 + a_2 z^{-1} + \cdots + a_{n+1} z^{-n}} \tag{5}$$

The **b** and **a** coefficients were determined based on a desired design point. In this case that design point is based on a desired cutoff frequency, ω_{3dB}. Using a filter design algorithm, a fourth order filter with a .88 Hz cutoff frequency (pass band of 1 Hz, stop band of .5 Hz) was designed. For this design, **b** and **a** have been determined as,

$$\mathbf{b} = \begin{pmatrix} .9855 & -3.9421 & 5.9132 & -3.9421 & .9855 \end{pmatrix}^T \tag{6}$$

$$\mathbf{a} = \begin{pmatrix} 1 & -3.9708 & 5.9129 & -3.9134 & .9713 \end{pmatrix}^T \tag{7}$$

So,

$$H(z) = \frac{.9855 - 3.9421z^{-1} + 5.9132z^{-2} - 3.9421z^{-3} + .9855z^{-4}}{1 - 3.9708z^{-1} + 5.9129z^{-2} - 3.9134z^{-3} + .9713z^{-4}} \tag{8}$$

The frequency response of this filter is displayed in *Figure 4*.

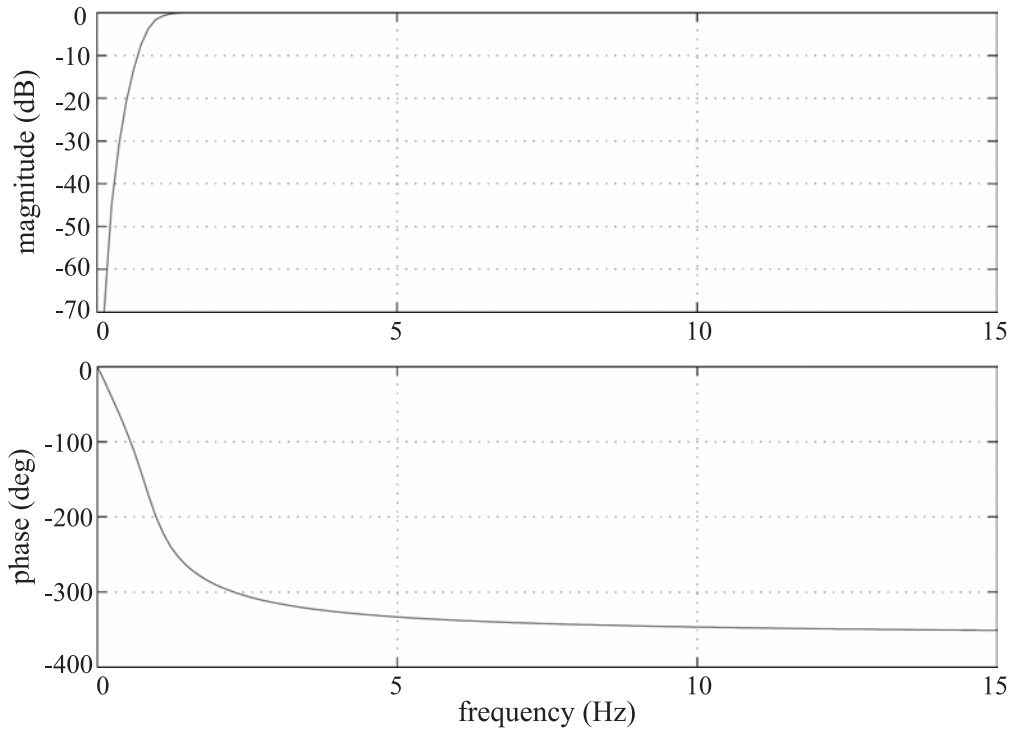

Figure 4. Frequency response of a high pass Butterworth filter designed to remove low frequency integration drift while preserving the higher frequency elements of the signal.

The Butterworth filter, described above, was employed in both the forward and reverse directions to generate *zero*-phase distortion. *Section 5.2* contains the results of this digital filtering which was used in conjunction with numerical integration to obtain the RV trajectory.

4 Reconstruction of Body Orientation

4.1 Algorithm

The task of determining the orientation history of an RV requires a knowledge of the gyroscope data. *Figure 5* depicts an incremental change in a body's orientation in $\mathbb{R}^3$. The incremental spin, $\Delta\theta$, about an axis, $\hat{\mathbf{k}}$, can be related to the instantaneous angular velocity, ω, of the body. We can use quaternions as an efficient means of representing orientation resulting from incremental motion. *Appendix A* provides an overview of the relevant spherical kinematics with coverage of quaternions (*A.4*) and the calculus of rotations (*A.5*).

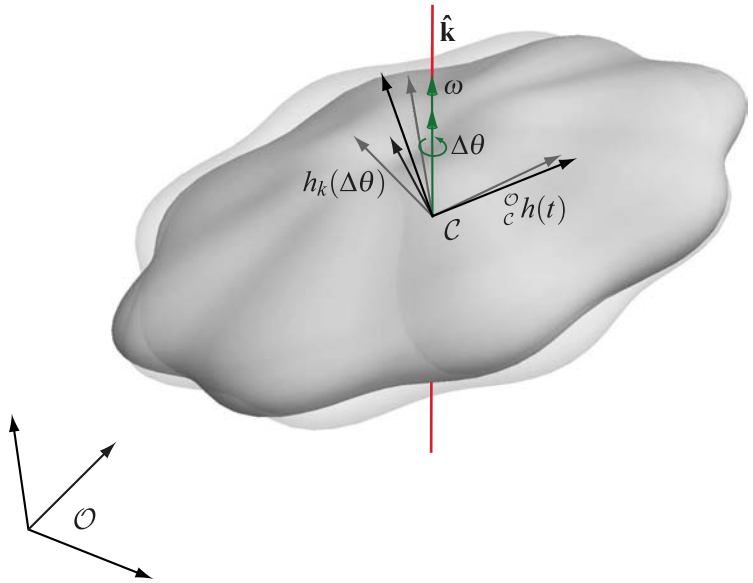

Figure 5. Instantaneous spin of a body about an axis. The incremental spin, $\Delta\theta$, about an axis, $\hat{\mathbf{k}}$, can be related to the instantaneous angular velocity, ω, of the body.

Since the gyroscopes provide angular velocity in the body's local reference frame we can approximate the orientation quaternion, $\overset{\mathcal{O}}{\mathcal{C}}h(t+\Delta t)$, of the body based on the previous orientation, $\overset{\mathcal{O}}{\mathcal{C}}h(t)$, and the incremental quaternion, h_k, associated with a finite but small incremental rotation, $\Delta\theta$, about an axis, $\hat{\mathbf{k}}$, that is fixed during the rotation. This can be expressed as,

$$\overset{\mathcal{O}}{\mathcal{C}}h(t+\Delta t) \approxeq \overset{\mathcal{O}}{\mathcal{C}}h(t)h_k(\Delta\theta) \tag{9}$$

Note that the spin axis of the incremental rotation is represented in the local body frame in (9) as opposed to the base frame (as in *Appendix A.5.2*) since the gyroscopes measure angular velocity in the local body frame. Due to small angle properties (see *Appendix A.5.2*),

$$h_k(\Delta\theta) \approxeq 1 + k_x\frac{\Delta\theta}{2}\mathbf{i} + k_y\frac{\Delta\theta}{2}\mathbf{j} + k_z\frac{\Delta\theta}{2}\mathbf{k} = 1 + \frac{1}{2}\omega\Delta t \tag{10}$$

where ω is the angular velocity quaternion,

$$\omega = 0 + \omega_x\mathbf{i} + \omega_y\mathbf{j} + \omega_z\mathbf{k} \tag{11}$$

Thus, for numerical integration we can use the following relationship,

$$ {}^{\mathcal{O}}_{\mathcal{C}}h(t+\Delta t) \approxeq {}^{\mathcal{O}}_{\mathcal{C}}h(t)\left(1+\frac{\omega_x\Delta t}{2}\mathbf{i}+\frac{\omega_y\Delta t}{2}\mathbf{j}+\frac{\omega_z\Delta t}{2}\mathbf{k}\right) \tag{12} $$

If we had implemented this integration using orthogonal rotation matrices we would have,

$$ {}^{\mathcal{O}}_{\mathcal{C}}\mathbf{Q}(t+\Delta t) \approxeq {}^{\mathcal{O}}_{\mathcal{C}}\mathbf{Q}(t)\begin{pmatrix} 1 & -\omega_z & \omega_y \\ \omega_z & 1 & -\omega_x \\ -\omega_y & \omega_x & 1 \end{pmatrix}\Delta t \tag{13} $$

However, the orthogonality properties of ${}^{\mathcal{O}}_{\mathcal{C}}\mathbf{Q}(t)$ would degrade with successive multiplications at finite precision, causing significant problems. In the case of the unit quaternion relationship of (12) the only concern would be that the length of the quaternion would deviate from unity with successive multiplications. This could be easily corrected by renormalizing the quaternion as,

$$ {}^{\mathcal{O}}_{\mathcal{C}}h(t+\Delta t) \approxeq \frac{{}^{\mathcal{O}}_{\mathcal{C}}h(t)\left(1+\frac{1}{2}\omega\Delta t\right)}{\left\|{}^{\mathcal{O}}_{\mathcal{C}}h(t)\left(1+\frac{1}{2}\omega\Delta t\right)\right\|} \tag{14} $$

It is also useful to represent the orientation in terms of Euler angles. We can convert from quaternions to rotation matrices using the following relationship,

$$ \mathbf{Q}(h) = \begin{pmatrix} 2(h_0h_0+h_1h_1)-1 & 2(h_1h_2-h_0h_3) & 2(h_1h_3+h_0h_2) \\ 2(h_1h_2+h_0h_3) & 2(h_0h_0+h_2h_2)-1 & 2(h_2h_3-h_0h_1) \\ 2(h_1h_3-h_0h_2) & 2(h_2h_3+h_0h_1) & 2(h_0h_0+h_3h_3)-1 \end{pmatrix} \tag{15} $$

We can then convert from $\mathbf{Q}(h)$ to an *xyz* Euler set, $\{\alpha,\beta,\gamma\}$, using the solution for *xzx* Euler angles in terms of the components of $\mathbf{Q}$, (see *Appendix A.3*). First we note,

$$ \mathbf{Q}_{xzx}(\alpha,\beta,\gamma) = \begin{pmatrix} \cos\beta & -\sin\beta\cos\gamma & \sin\beta\sin\gamma \\ \cos\alpha\sin\beta & \cos\alpha\cos\beta\cos\gamma-\sin\alpha\sin\gamma & -\cos\alpha\cos\beta\sin\gamma-\sin\alpha\cos\gamma \\ \sin\alpha\sin\beta & \sin\alpha\cos\beta\cos\gamma+\cos\alpha\sin\gamma & -\sin\alpha\cos\beta\sin\gamma+\cos\alpha\cos\gamma \end{pmatrix} \tag{16} $$

The inverse solution is then,

If $\sin\beta \neq 0$, $(\beta \neq 0,\pi)$,

$$ \beta = \text{Atan2}(\sqrt{Q_{21}^2+Q_{31}^2}, Q_{11}) \tag{17} $$

$$ \alpha = \text{Atan2}(Q_{31}/s\beta, Q_{21}/s\beta) \tag{18} $$

$$ \gamma = \text{Atan2}(Q_{13}/s\beta, -Q_{12}/s\beta) \tag{19} $$

If $\beta = 0$,

$$ \alpha = 0 \tag{20} $$

$$ \gamma = \text{Atan2}(Q_{32}, Q_{22}) \tag{21} $$

If $\beta = \pi$,

$$ \alpha = 0 \tag{22} $$

$$ \gamma = \text{Atan2}(Q_{32}, -Q_{22}) \tag{23} $$

4.2 Results

Figure 6 displays plots of quaternion data calculated from gyroscope data. The data was calculated using the algorithm described in *Section 4.1*. The quaternion elements h_2 and h_3 are of special interest since they encode the k_y and k_z components of the spin axis, $\hat{\mathbf{k}}$. These components correspond to the lateral axes of the RV. While unit quaternions possess computational efficacy, Euler angles can provide an easier means of mentally decomposing the orientation of a body from 2-D plots. *Figure 7* displays a plot of the *xzx* Euler angles associated with the RV orientation. Of these angles, β is of particular interest since it indicates the angular displacement between the RV main axis and the base coordinate frame *x*-axis. The β angle can also be related to the coning angle of the RV (to be discussed in *Section 5.1*).

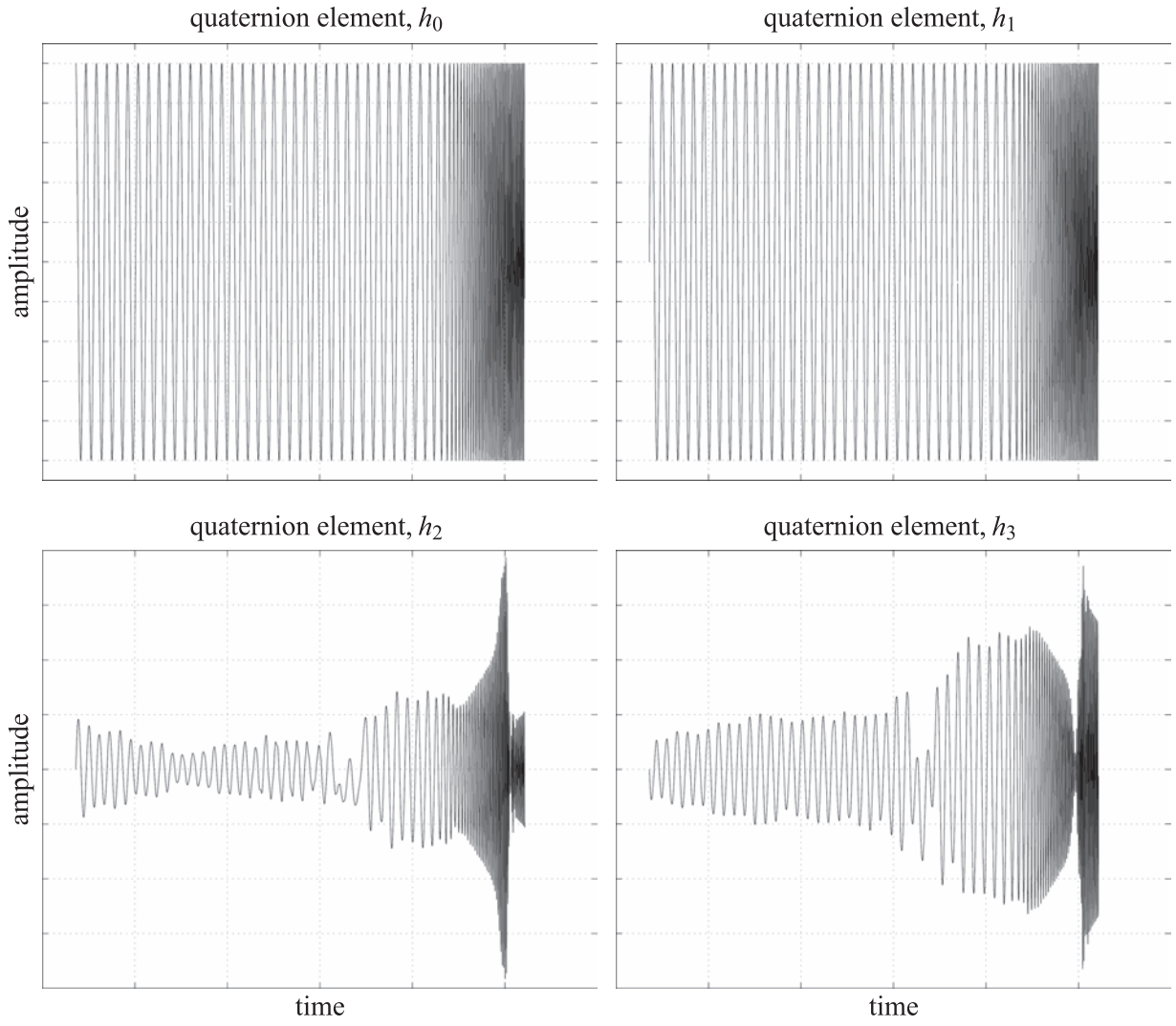

Figure 6. Quaternion time history derived from integration of the gyroscope data. The four quaternion components are displayed. Units have been intentionally omitted.

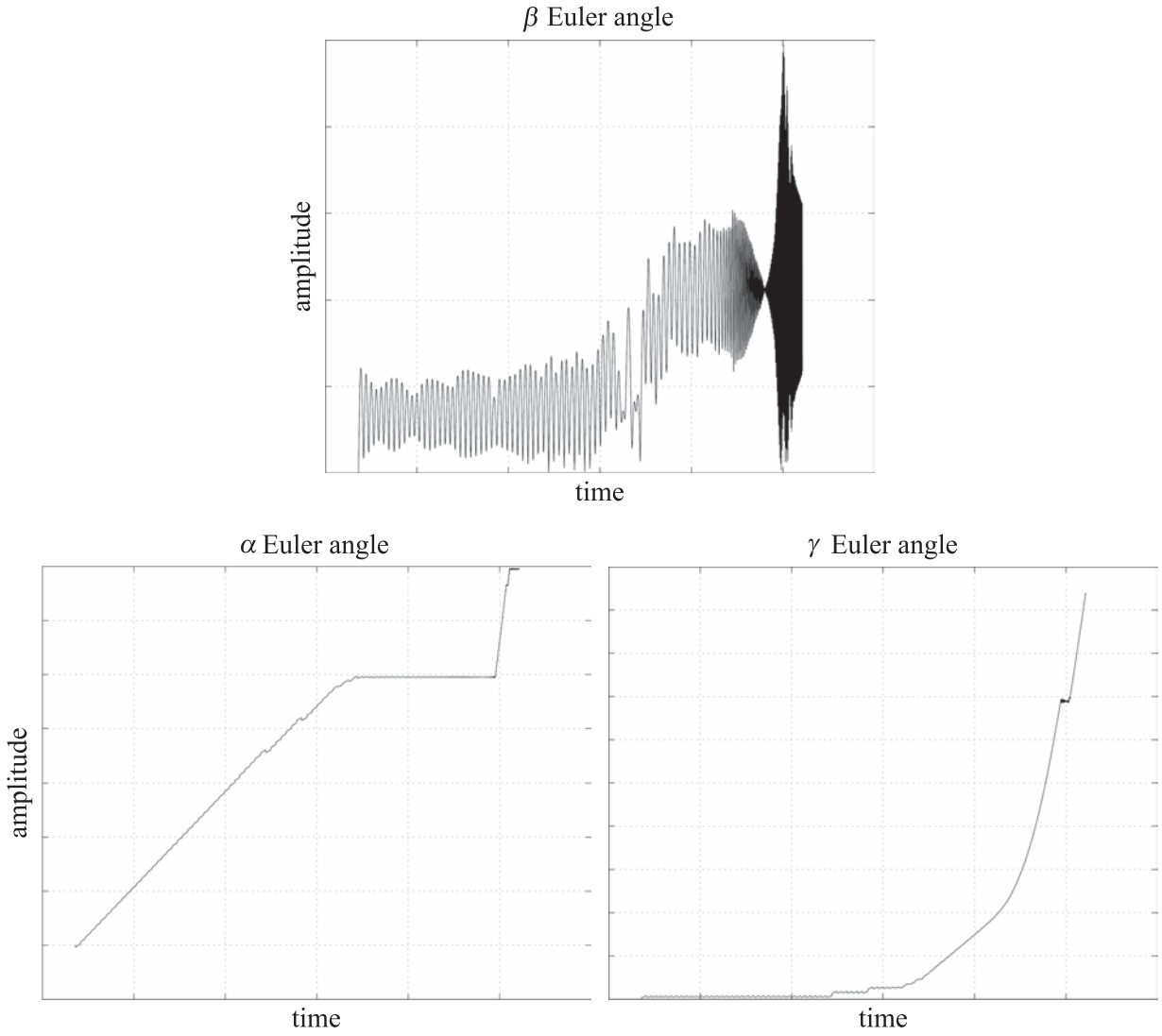

Figure 7. Euler angle time history derived from integration of the gyroscope data. The three Euler angles are displayed. Units have been intentionally omitted.

5 Reconstruction of Center of Mass Trajectory

5.1 Algorithm

The task of determining the motion history of the center of mass of an RV requires a knowledge of the body's initial conditions, and the gyroscope and accelerometer data. *Figure 8* depicts a configuration where an accelerometer is mounted in each of three locations (frames 1, 2, and 3).

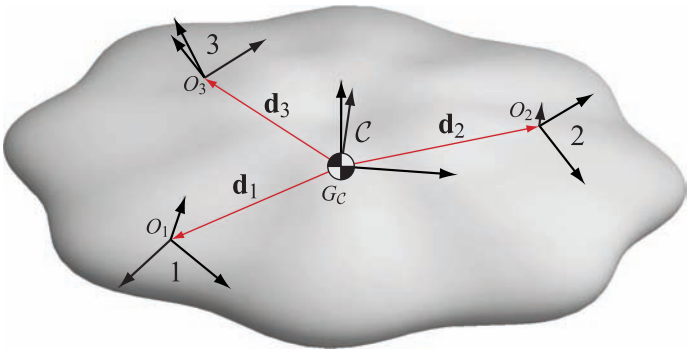

Figure 8. Body with acceleration components known at three different locations. Accelerometer data taken at three different locations and gyroscope data for the body can be used to determine the acceleration of the center of mass.

The following relationships exist between the acceleration of the center of mass and the accelerations of the accelerometer frames,

$$ {}^{\mathcal{C}}\mathbf{a}_{O_1} = {}^{\mathcal{C}}_{1}\mathbf{Q}\,{}^{1}\mathbf{a}_{O_1} = {}^{\mathcal{C}}\mathbf{a}_{G_\mathcal{C}} + {}^{\mathcal{C}}\omega_\mathcal{C} \times ({}^{\mathcal{C}}\omega_\mathcal{C} \times {}^{\mathcal{C}}\mathbf{d}_1) + {}^{\mathcal{C}}\alpha_\mathcal{C} \times {}^{\mathcal{C}}\mathbf{d}_1 \tag{24} $$

$$ {}^{\mathcal{C}}\mathbf{a}_{O_2} = {}^{\mathcal{C}}_{2}\mathbf{Q}\,{}^{2}\mathbf{a}_{O_2} = {}^{\mathcal{C}}\mathbf{a}_{G_\mathcal{C}} + {}^{\mathcal{C}}\omega_\mathcal{C} \times ({}^{\mathcal{C}}\omega_\mathcal{C} \times {}^{\mathcal{C}}\mathbf{d}_2) + {}^{\mathcal{C}}\alpha_\mathcal{C} \times {}^{\mathcal{C}}\mathbf{d}_2 \tag{25} $$

$$ {}^{\mathcal{C}}\mathbf{a}_{O_3} = {}^{\mathcal{C}}_{3}\mathbf{Q}\,{}^{3}\mathbf{a}_{O_3} = {}^{\mathcal{C}}\mathbf{a}_{G_\mathcal{C}} + {}^{\mathcal{C}}\omega_\mathcal{C} \times ({}^{\mathcal{C}}\omega_\mathcal{C} \times {}^{\mathcal{C}}\mathbf{d}_3) + {}^{\mathcal{C}}\alpha_\mathcal{C} \times {}^{\mathcal{C}}\mathbf{d}_3 \tag{26} $$

These three vector equations yield nine scalar equations and nine unknowns. The nine unknowns include the center of mass acceleration components, ${}^{\mathcal{C}}\ddot{x}_{G_\mathcal{C}}$, ${}^{\mathcal{C}}\ddot{y}_{G_\mathcal{C}}$, and ${}^{\mathcal{C}}\ddot{z}_{G_\mathcal{C}}$, as well as the six acceleration components of frames 1, 2, and 3 which lie in directions orthogonal to the accelerometers. The other three acceleration components of frames 1, 2, and 3 are known explicitly from the accelerometer values, a_1, a_2, and a_3. For a general formulation where the accelerometers are mounted arbitrarily we have a linear system, $\mathbf{Ax} = \mathbf{b}$, at a given instant of time where $\mathbf{A}$ is defined as,

$$ \mathbf{A} \triangleq \begin{pmatrix} \mathbf{1} & -{}^{\mathcal{C}}_{1}\mathbf{Q} & \mathbf{0} & \mathbf{0} \\ \mathbf{1} & \mathbf{0} & -{}^{\mathcal{C}}_{2}\mathbf{Q} & \mathbf{0} \\ \mathbf{1} & \mathbf{0} & \mathbf{0} & -{}^{\mathcal{C}}_{3}\mathbf{Q} \\ \mathbf{0} & \mathrm{diag}(\hat{\mathbf{e}}_1)\mathbf{N} & \mathrm{diag}(\hat{\mathbf{e}}_2)\mathbf{N} & \mathrm{diag}(\hat{\mathbf{e}}_3)\mathbf{N} \end{pmatrix} \tag{27} $$

and $\mathbf{N}$ is a logical matrix defined as,

$$ N_{ij} \triangleq \begin{cases} 1 & \text{if accelerometer } i \text{ measures in the } j \text{ direction} \\ 0 & \text{if accelerometer } i \text{ does not measures in the } j \text{ direction} \end{cases} \tag{28} $$

The vectors $\mathbf{x}$ and $\mathbf{b}$ are defined as,

$$\mathbf{x} \triangleq \begin{pmatrix} {}^{\mathcal{C}}\mathbf{a}_{G_{\mathcal{C}}} \\ {}^{1}\mathbf{a}_{O_1} \\ {}^{2}\mathbf{a}_{O_2} \\ {}^{3}\mathbf{a}_{O_3} \end{pmatrix} \quad \text{and,} \quad \mathbf{b} \triangleq \begin{pmatrix} -{}^{\mathcal{C}}\omega_{\mathcal{C}} \times ({}^{\mathcal{C}}\omega_{\mathcal{C}} \times {}^{\mathcal{C}}\mathbf{d}_1) - {}^{\mathcal{C}}\alpha_{\mathcal{C}} \times {}^{\mathcal{C}}\mathbf{d}_1 \\ -{}^{\mathcal{C}}\omega_{\mathcal{C}} \times ({}^{\mathcal{C}}\omega_{\mathcal{C}} \times {}^{\mathcal{C}}\mathbf{d}_2) - {}^{\mathcal{C}}\alpha_{\mathcal{C}} \times {}^{\mathcal{C}}\mathbf{d}_2 \\ -{}^{\mathcal{C}}\omega_{\mathcal{C}} \times ({}^{\mathcal{C}}\omega_{\mathcal{C}} \times {}^{\mathcal{C}}\mathbf{d}_3) - {}^{\mathcal{C}}\alpha_{\mathcal{C}} \times {}^{\mathcal{C}}\mathbf{d}_3 \\ \mathbf{a} \end{pmatrix} \tag{29}$$

where $\mathbf{a} \triangleq \begin{pmatrix} a_1 & a_2 & a_3 \end{pmatrix}^T$ is the vector of accelerometer values. Because the accelerometers are typically aligned with the center of mass coordinate frame, the above system can be reduced to three scalar equations and three unknowns. For example, we will be dealing with a case where the accelerometer for frame 1 measures in the $+x$-axis of the center of mass frame, the accelerometer for frame 2 measures in the $+y$-axis, and the accelerometer for frame 3 measures in the $-z$-axis. So we have,

$${}^{\mathcal{C}}\ddot{x}_{G_{\mathcal{C}}} = a_1 - [{}^{\mathcal{C}}\omega_{\mathcal{C}} \times ({}^{\mathcal{C}}\omega_{\mathcal{C}} \times {}^{\mathcal{C}}\mathbf{d}_1) + {}^{\mathcal{C}}\alpha_{\mathcal{C}} \times {}^{\mathcal{C}}\mathbf{d}_1] \cdot \hat{\mathbf{e}}_1 \tag{30}$$

$${}^{\mathcal{C}}\ddot{y}_{G_{\mathcal{C}}} = a_2 - [{}^{\mathcal{C}}\omega_{\mathcal{C}} \times ({}^{\mathcal{C}}\omega_{\mathcal{C}} \times {}^{\mathcal{C}}\mathbf{d}_2) + {}^{\mathcal{C}}\alpha_{\mathcal{C}} \times {}^{\mathcal{C}}\mathbf{d}_2] \cdot \hat{\mathbf{e}}_2 \tag{31}$$

$${}^{\mathcal{C}}\ddot{z}_{G_{\mathcal{C}}} = -a_3 - [{}^{\mathcal{C}}\omega_{\mathcal{C}} \times ({}^{\mathcal{C}}\omega_{\mathcal{C}} \times {}^{\mathcal{C}}\mathbf{d}_3) + {}^{\mathcal{C}}\alpha_{\mathcal{C}} \times {}^{\mathcal{C}}\mathbf{d}_3] \cdot \hat{\mathbf{e}}_3 \tag{32}$$

Transforming into the initial world coordinate frame $\mathcal{O}$, using quaternions, we have,

$${}^{\mathcal{O}}a_{G_{\mathcal{C}}} = {}^{\mathcal{O}}_{\mathcal{C}}h \, {}^{\mathcal{C}}a_{G_{\mathcal{C}}} \, {}^{\mathcal{C}}_{\mathcal{O}}h \tag{33}$$

It is noted that in the case above which involves quaternion operations, a is taken to be an acceleration quaternion of the form $a = 0 + a_x\mathbf{i} + a_y\mathbf{j} + a_z\mathbf{k}$. For numerical integration we can use the following trapezoidal relationships,

$${}^{\mathcal{O}}\mathbf{v}_{G_{\mathcal{C}}}(t+\Delta t) \approxeq {}^{\mathcal{O}}\mathbf{v}_{G_{\mathcal{C}}}(t) + \frac{1}{2}\left[{}^{\mathcal{O}}\mathbf{a}_{G_{\mathcal{C}}}(t) + {}^{\mathcal{O}}\mathbf{a}_{G_{\mathcal{C}}}(t+\Delta t)\right]\Delta t \tag{34}$$

$${}^{\mathcal{O}}\mathbf{r}_{G_{\mathcal{C}}}(t+\Delta t) \approxeq {}^{\mathcal{O}}\mathbf{r}_{G_{\mathcal{C}}}(t) + \frac{1}{2}\left[{}^{\mathcal{O}}\mathbf{v}_{G_{\mathcal{C}}}(t) + {}^{\mathcal{O}}\mathbf{v}_{G_{\mathcal{C}}}(t+\Delta t)\right]\Delta t \tag{35}$$

Having computed the center of mass trajectory and body orientation history, we can calculate the coning angle of the RV over the time series. *Figure 9* depicts the combined orientation and position information describing the body's motion in $\mathbb{R}^3$. The coning angle, φ, is defined as the angle between the RV x-axis and the tangent to the trajectory at a given instant of time.

Using the results of *Section 4.1* we know the α and β Euler angles of the RV orientation. The RV x-axis unit vector in the base coordinate frame is thus,

$$\mathbf{u}_x = \begin{pmatrix} \cos\beta \\ \cos\alpha\sin\beta \\ \sin\alpha\sin\beta \end{pmatrix} \tag{36}$$

Alternately, this vector can be expressed as the first column of $\mathbf{Q}$,

$$\mathbf{u}_x = \mathbf{Q}\hat{\mathbf{e}}_1 = \begin{pmatrix} 2(h_0h_0 + h_1h_1) - 1 \\ 2(h_1h_2 + h_0h_3) \\ 2(h_1h_3 - h_0h_2) \end{pmatrix} \tag{37}$$

The tangent to the trajectory is,

$$\mathbf{u}_{\text{traj}} = \frac{\Delta\mathbf{r}_{G_{\mathcal{C}}}}{\left\|\Delta\mathbf{r}_{G_{\mathcal{C}}}\right\|} \tag{38}$$

so,

$$\cos\varphi = \mathbf{u}_x \cdot \mathbf{u}_{\text{traj}} \tag{39}$$

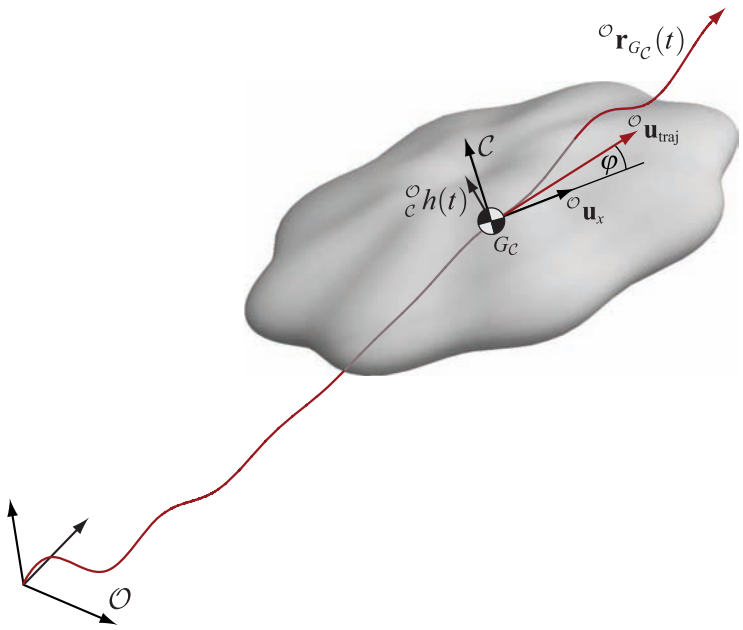

Figure 9. Center of mass position time history and orientation time history relative to a world frame. The coning angle, φ, is shown as the angle between body axis, $\mathbf{u}_x$, and the path trajectory, $\mathbf{u}_{\text{traj}}$.

5.2 Results

Figure 10 displays plots of the center of mass acceleration components derived from telemetry data, using the algorithm described in *Section 5.1*. *Figure 11* displays plots of the center of mass velocity and position in the *x* direction.

Figure 12 displays plots of the center of mass velocity and position in the *y* direction. The signals were conditioned with a high pass filter as described in *Section 3.3*. The power spectral density (PSD) of the signals is also shown in *Figure 12*. This indicates the dominant frequency range of the signals after filtering. It can be seen that the signals have been attenuated at the lowest frequencies due to the filtering employed. *Figure 13* displays plots of the center of mass velocity and position in the *z* direction. Again, the power spectral densities of the signals are shown. After final conditioning of the integrated signals a trajectory was generated. *Figure 14* displays the center of mass trajectory of the RV. The scale in the *x* direction is greatly compressed. The coning angle was calculated using the algorithm described in *Section 5.1*. *Figure 15* displays a plot of the coning angle.

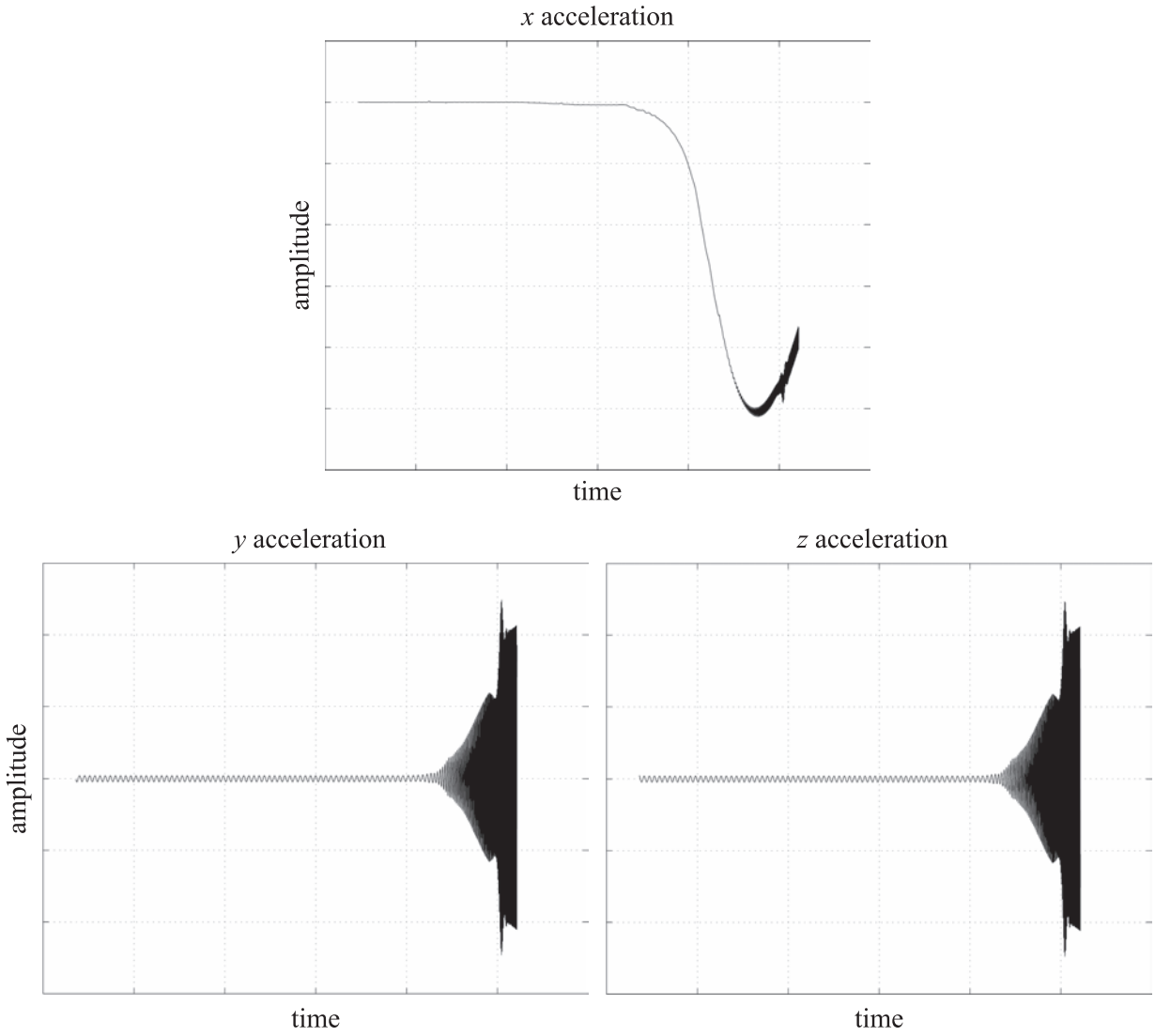

Figure 10. Center of mass acceleration components derived from gyroscope and accelerometer data. Units have been intentionally omitted.

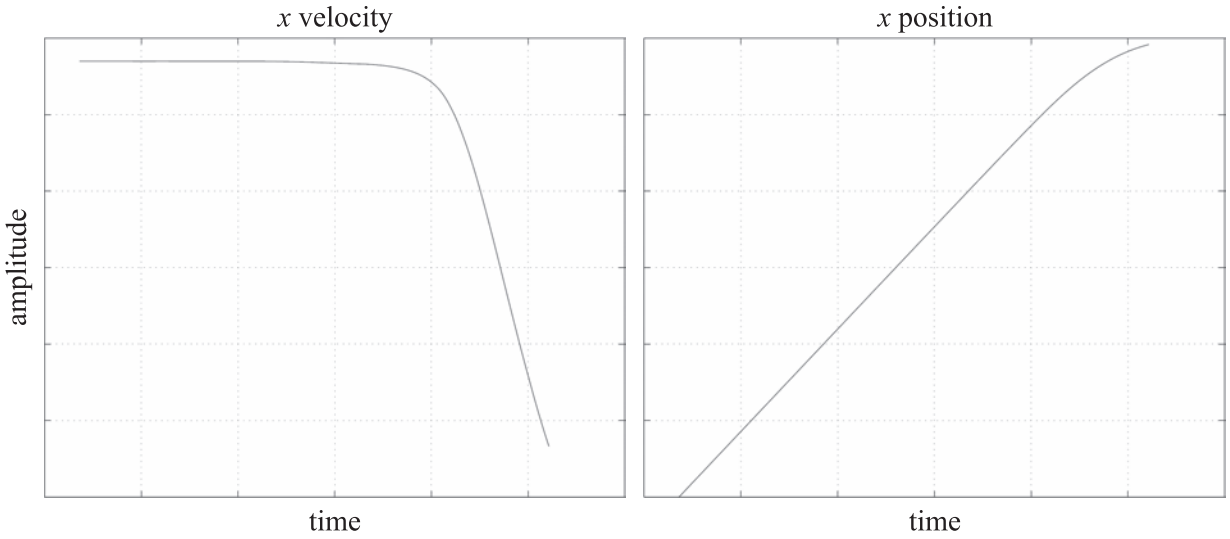

Figure 11. Center of mass velocity and position *x* components. Numerical integration was performed on the acceleration data. Units have been intentionally omitted.

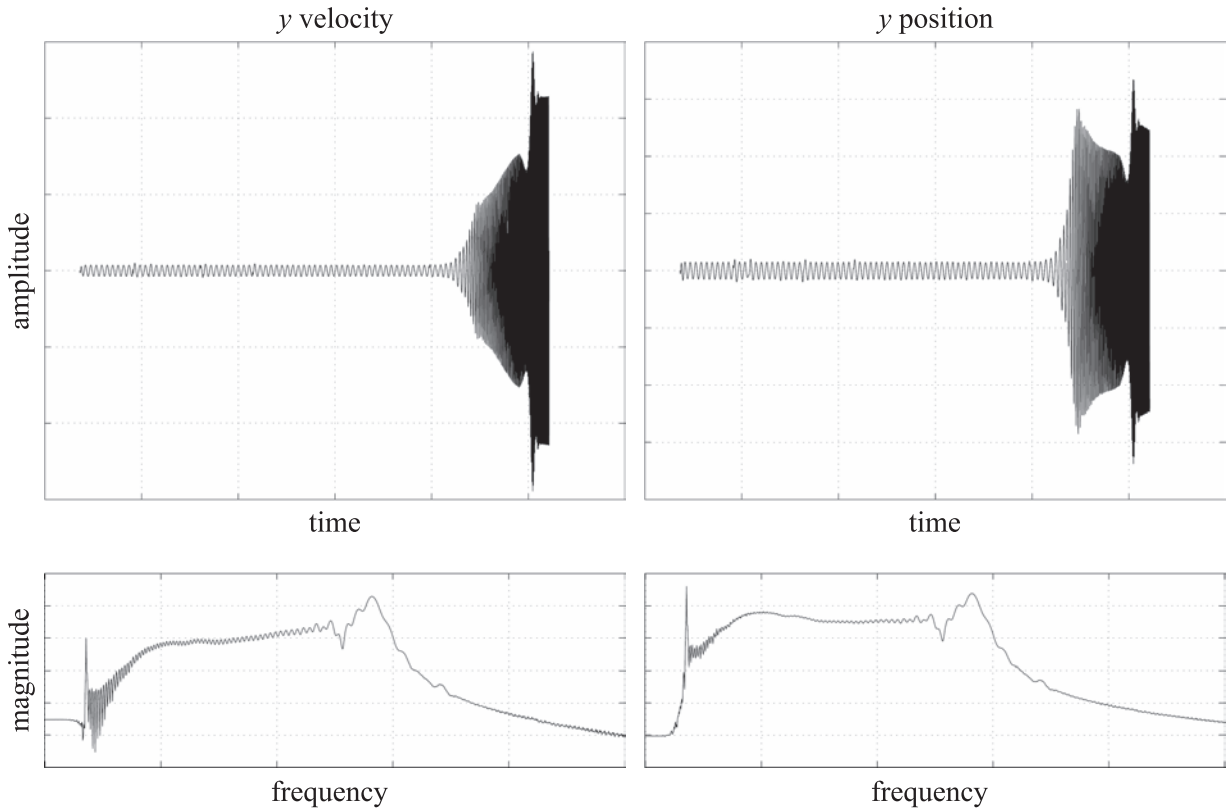

Figure 12. Center of mass velocity and position *y* components. (Top) The integrated signals were conditioned with a high pass filter. (Bottom) The power spectral density of the signals after filtering. Units have been intentionally omitted.

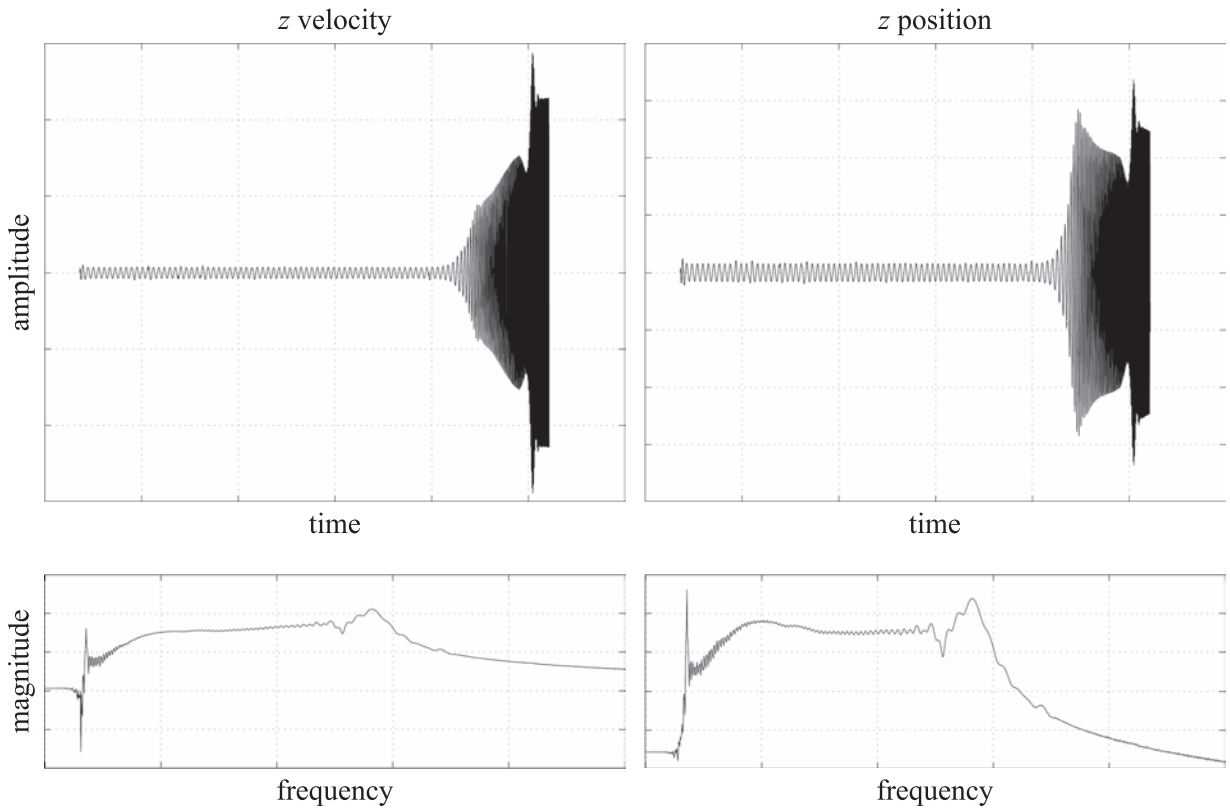

Figure 13. Center of mass velocity and position z components. (Top) The integrated signals were conditioned with a high pass filter. (Bottom) The power spectral density of the signals after filtering. Units have been intentionally omitted.

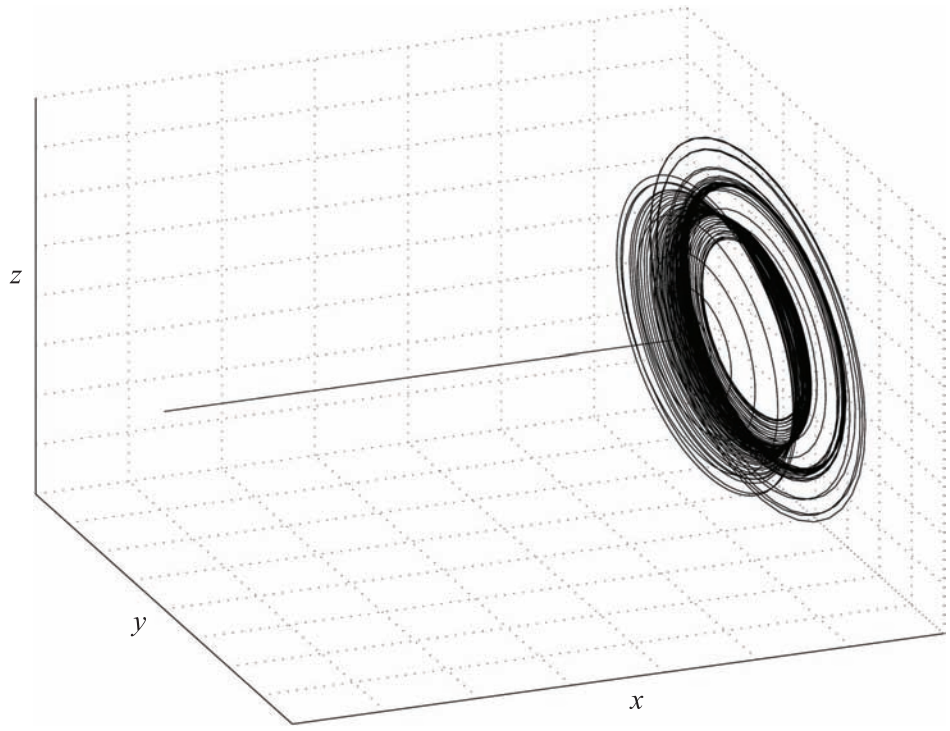

Figure 14. RV trajectory generated after final conditioning of the integrated signals. The scale in the x direction is greatly compressed. Units have been intentionally omitted.

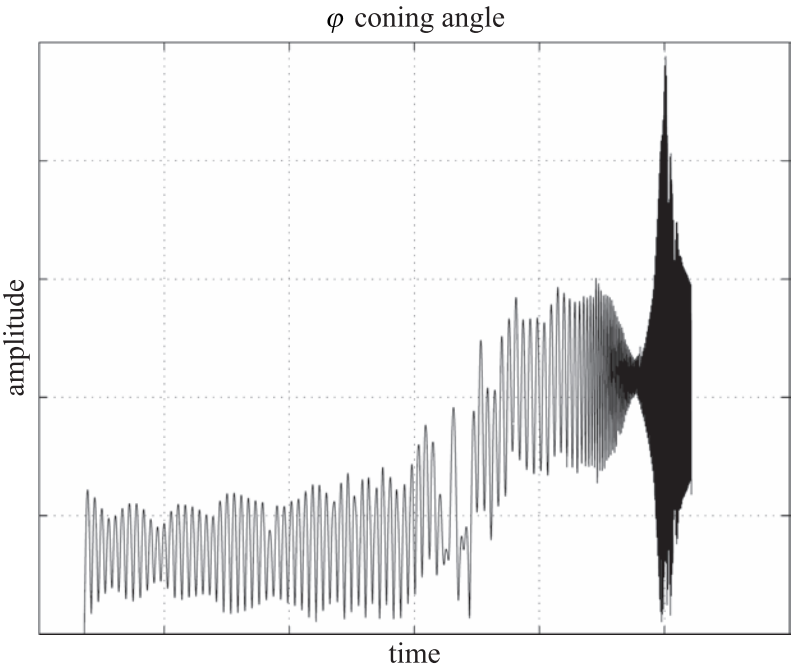

Figure 15. Coning angle of the RV determined from the quaternion orientation history and the path trajectory. Units have been intentionally omitted.

6 Conclusion

We have presented an approach and numerical implementation for the reconstruction of re-entry vehicle motion solely from gyroscope and accelerometer data. This makes use of quaternions as a computationally efficient tool for encoding body orientation, and changes in orientation, in three dimensions. In addition to signal processing and data conditioning procedures the numerical approaches included algorithms for numerical quaternion-based integration of gyroscope data to yield orientation history, as well as accelerometer triangulation to determine the acceleration of the RV center of mass frame and numerical integration to yield the RV trajectory. The algorithms have been implemented in MATLAB [10] and C++ [3]. Actual flight data was processed and presented to demonstrate the implementation of these methods.

References

[1] A. E. Bryson. *Control of Spacecraft and Aircraft*. Princeton University Press, Princeton, 1994.

[2] J.J. Craig. *Introduction to Robotics: Mechanics and Control*. Addison Wesley, New York, third edition, 2004.

[3] V. De Sapio. KDL++: An object-oriented kinematics & dynamics library in C++. SAND Report SAND2000-8207, Sandia National Laboratories, 2000.

[4] F. Franklin, J. D. Powell, and M. L. Workman. *Digital Control of Dynamic Systems*. Addison Wesley, New York, third edition, 1997.

[5] H. Goldstein, C Poole, and J. Safko. *Classical Mechanics*. Addison Wesley, New York, third edition, 2002.

[6] W. R. Hamilton. *Elements of Quaternions*. Longmans, Green, and Co., London, 1866.

[7] J. C. Hart, G. K. Francis, and L. H. Kauffman. Visualizing quaternion rotation. *ACM Transactions on Graphics (TOG)*, 13(3):256–276, 1994.

[8] T. R. Kane, P. W. Likins, and D. A. Levinson. *Spacecraft Dynamics*. Mc Graw-Hill, New York, 1983.

[9] J. B. Kuipers. *Quaternions and Rotation Sequences: A Primer with Applications to Orbits, Aerospace and Virtual Reality*. Princeton University Press, Princeton, 2002.

[10] MATLAB. http://www.mathworks.com.

[11] F. C. Moon. *Applied Dynamics: with Applications to Multibody and Mechatronic Systems*. Wiley, New York, second edition, 2008.

A Spherical Kinematics

Spherical kinematics is concerned with the special orthogonal group $SO(3)$. This group is defined as the set of all proper orthogonal matrices, $\mathbf{Q}$.

$$SO(3) = \{\mathbf{Q} \,|\, \mathbf{Q} \in \mathbb{R}^{3\times 3}, \mathbf{Q}^T\mathbf{Q} = \mathbf{Q}\mathbf{Q}^T = \mathbf{1}\} \tag{40}$$

The orthogonal rotation matrix, $\mathbf{Q}$, will be described in the following sections, as well as some other ways to parameterize rotation. These include angle-sets, axis-angle parameters, and unit quaternions.

A.1 Orthogonal Rotation Matrices

Orthogonal rotation matrices encode spatial rotation by describing the orientation of one coordinate frame relative to another. The column vectors of a rotation matrix are the base vectors of the coordinate frame of interest, expressed within an embedding frame. For example, *Figure A.1* depicts frame $\mathcal{B}$ rotated relative to frame $\mathcal{A}$.

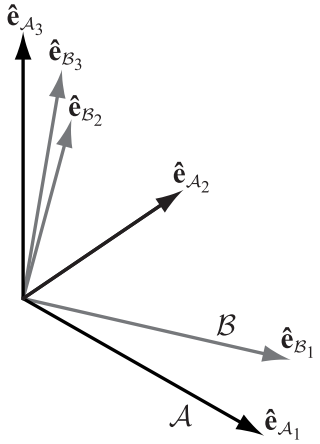

Figure A.1. Rotation of frame $\mathcal{B}$ relative to frame $\mathcal{A}$. The base vectors $\hat{\mathbf{e}}_{\mathcal{B}_1}$, $\hat{\mathbf{e}}_{\mathcal{B}_2}$, and $\hat{\mathbf{e}}_{\mathcal{B}_3}$ are expressed within the embedding frame $\mathcal{A}$ to yield the orthogonal rotation matrix, ${}^{\mathcal{A}}_{\mathcal{B}}\mathbf{Q}$.

The rotation matrix describing the orientation of frame $\mathcal{B}$ in frame $\mathcal{A}$ is,

$${}^{\mathcal{A}}_{\mathcal{B}}\mathbf{Q} = \begin{pmatrix} \uparrow & \uparrow & \uparrow \\ {}^{\mathcal{A}}\hat{\mathbf{e}}_{\mathcal{B}_1} & {}^{\mathcal{A}}\hat{\mathbf{e}}_{\mathcal{B}_2} & {}^{\mathcal{A}}\hat{\mathbf{e}}_{\mathcal{B}_3} \\ \downarrow & \downarrow & \downarrow \end{pmatrix} = \begin{pmatrix} \hat{\mathbf{e}}_{\mathcal{B}_1}\cdot\hat{\mathbf{e}}_{\mathcal{A}_1} & \hat{\mathbf{e}}_{\mathcal{B}_2}\cdot\hat{\mathbf{e}}_{\mathcal{A}_1} & \hat{\mathbf{e}}_{\mathcal{B}_3}\cdot\hat{\mathbf{e}}_{\mathcal{A}_1} \\ \hat{\mathbf{e}}_{\mathcal{B}_1}\cdot\hat{\mathbf{e}}_{\mathcal{A}_2} & \hat{\mathbf{e}}_{\mathcal{B}_2}\cdot\hat{\mathbf{e}}_{\mathcal{A}_2} & \hat{\mathbf{e}}_{\mathcal{B}_3}\cdot\hat{\mathbf{e}}_{\mathcal{A}_2} \\ \hat{\mathbf{e}}_{\mathcal{B}_1}\cdot\hat{\mathbf{e}}_{\mathcal{A}_3} & \hat{\mathbf{e}}_{\mathcal{B}_2}\cdot\hat{\mathbf{e}}_{\mathcal{A}_3} & \hat{\mathbf{e}}_{\mathcal{B}_3}\cdot\hat{\mathbf{e}}_{\mathcal{A}_3} \end{pmatrix} \tag{41}$$

For rotations about the principal axes,

$$\mathbf{Q}_x(\theta) = \begin{pmatrix} 1 & 0 & 0 \\ 0 & \cos\theta & -\sin\theta \\ 0 & \sin\theta & \cos\theta \end{pmatrix}, \mathbf{Q}_y(\theta) = \begin{pmatrix} \cos\theta & 0 & \sin\theta \\ 0 & 1 & 0 \\ -\sin\theta & 0 & \cos\theta \end{pmatrix}$$
$$\mathbf{Q}_z(\theta) = \begin{pmatrix} \cos\theta & -\sin\theta & 0 \\ \sin\theta & \cos\theta & 0 \\ 0 & 0 & 1 \end{pmatrix} \tag{42}$$

The inverse of a rotation matrix, $\mathbf{Q}^{-1}$, satisfies

$$\mathbf{Q}\mathbf{Q}^{-1} = \mathbf{Q}^{-1}\mathbf{Q} = \mathbf{1} = \begin{pmatrix} 1 & 0 & 0 \\ 0 & 1 & 0 \\ 0 & 0 & 1 \end{pmatrix} \tag{43}$$

Since $\mathbf{Q}$ is an orthogonal matrix,

$${}^{\mathcal{A}}_{\mathcal{B}}\mathbf{Q}^T\,{}^{\mathcal{A}}_{\mathcal{B}}\mathbf{Q} = \begin{pmatrix} \leftarrow & {}^{\mathcal{A}}\hat{\mathbf{e}}^T_{\mathcal{B}_1} & \rightarrow \\ \leftarrow & {}^{\mathcal{A}}\hat{\mathbf{e}}^T_{\mathcal{B}_2} & \rightarrow \\ \leftarrow & {}^{\mathcal{A}}\hat{\mathbf{e}}^T_{\mathcal{B}_3} & \rightarrow \end{pmatrix} \begin{pmatrix} \uparrow & \uparrow & \uparrow \\ {}^{\mathcal{A}}\hat{\mathbf{e}}_{\mathcal{B}_1} & {}^{\mathcal{A}}\hat{\mathbf{e}}_{\mathcal{B}_2} & {}^{\mathcal{A}}\hat{\mathbf{e}}_{\mathcal{B}_3} \\ \downarrow & \downarrow & \downarrow \end{pmatrix} = \mathbf{1} \tag{44}$$

Therefore,

$${}^{\mathcal{B}}_{\mathcal{A}}\mathbf{Q}\,{}^{\mathcal{A}}_{\mathcal{B}}\mathbf{Q} = {}^{\mathcal{A}}_{\mathcal{B}}\mathbf{Q}^T\,{}^{\mathcal{A}}_{\mathcal{B}}\mathbf{Q} = {}^{\mathcal{A}}_{\mathcal{B}}\mathbf{Q}^{-1}\,{}^{\mathcal{A}}_{\mathcal{B}}\mathbf{Q} = \mathbf{1} \tag{45}$$

and,

$$\mathbf{Q}^T = \mathbf{Q}^{-1} \tag{46}$$

Rotational transformation can be accommodated with rotation matrices using the product,

$${}^{\mathcal{A}}\mathbf{v} = {}^{\mathcal{A}}_{\mathcal{B}}\mathbf{Q}\,{}^{\mathcal{B}}\mathbf{v} \tag{47}$$

Additionally, multiple rotations can be concatenated using multiplication.

$${}^{\mathcal{A}}_{\mathcal{C}}\mathbf{Q} = {}^{\mathcal{A}}_{\mathcal{B}}\mathbf{Q}\,{}^{\mathcal{B}}_{\mathcal{C}}\mathbf{Q} \tag{48}$$

A.2 Axis-Angle Scheme

We begin by noting the following Euler's theorem on rotation.

Theorem 1. *There exists a spin axis and angle for any arbitrary orientation in* $\mathbb{R}^3$.

The axis-angle representation specifies a spin axis, about which a coordinate frame is rotated by a specified angle. *Figure A.2* depicts an arbitrary rotation. The axis-angle parameters are the spin axis, $\hat{\mathbf{k}}$, and the spin angle, θ.

We wish to determine the rotation matrix, ${}^{\mathcal{A}}_{\mathcal{B}}\mathbf{Q}$, associated with the rotation depicted in *Figure A.2*, in terms of the axis-angle parameters. Let us start by defining orthonormal vectors $\hat{\mathbf{i}}$ and $\hat{\mathbf{j}}$ to be orthogonal to unit vector $\hat{\mathbf{k}}$. Let coordinate frame $\mathcal{K}$ be defined by the base vectors $\hat{\mathbf{i}}, \hat{\mathbf{j}}, \hat{\mathbf{k}}$. Let $\mathcal{K}'$ be the coordinate frame that $\mathcal{K}$ is rotated into. Then,

$${}^{\mathcal{A}}_{\mathcal{B}}\mathbf{Q} = \mathbf{Q}_k(\theta) = {}^{\mathcal{A}}_{\mathcal{K}}\mathbf{Q}\,{}^{\mathcal{K}}_{\mathcal{K}'}\mathbf{Q}\,{}^{\mathcal{K}'}_{\mathcal{B}}\mathbf{Q} \tag{49}$$

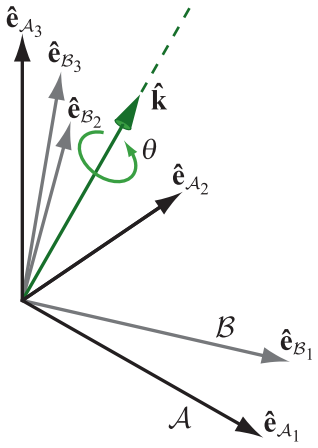

Figure A.2. The axis-angle scheme. A coordinate frame is rotated about a spin axis, $\hat{\mathbf{k}}$, by a specified angle, θ.

where,

$$\overset{\mathcal{A}}{\mathcal{K}}\mathbf{Q} = \begin{pmatrix} \uparrow & \uparrow & \uparrow \\ {}^{\mathcal{A}}\hat{\mathbf{i}} & {}^{\mathcal{A}}\hat{\mathbf{j}} & {}^{\mathcal{A}}\hat{\mathbf{k}} \\ \downarrow & \downarrow & \downarrow \end{pmatrix} = \begin{pmatrix} i_x & j_x & k_x \\ i_y & j_y & k_y \\ i_z & j_z & k_z \end{pmatrix} \tag{50}$$

and,

$$\overset{\mathcal{K}}{\mathcal{K}'}\mathbf{Q} = \mathbf{Q}_z(\theta) \tag{51}$$

and,

$$\overset{\mathcal{K}'}{\mathcal{B}}\mathbf{Q} = \overset{\mathcal{K}}{\mathcal{A}}\mathbf{Q} = \overset{\mathcal{A}}{\mathcal{K}}\mathbf{Q}^T \tag{52}$$

So,

$$\overset{\mathcal{A}}{\mathcal{B}}\mathbf{Q} = \mathbf{Q}_k(\theta) = \overset{\mathcal{A}}{\mathcal{K}}\mathbf{Q}\,\mathbf{Q}_z(\theta)\overset{\mathcal{K}}{\mathcal{A}}\mathbf{Q} \tag{53}$$

and,

$$\mathbf{Q}_k(\theta) = \begin{pmatrix} \uparrow & \uparrow & \uparrow \\ {}^{\mathcal{A}}\hat{\mathbf{i}} & {}^{\mathcal{A}}\hat{\mathbf{j}} & {}^{\mathcal{A}}\hat{\mathbf{k}} \\ \downarrow & \downarrow & \downarrow \end{pmatrix} \begin{pmatrix} \cos\theta & -\sin\theta & 0 \\ \sin\theta & \cos\theta & 0 \\ 0 & 0 & 1 \end{pmatrix} \begin{pmatrix} \leftarrow & {}^{\mathcal{A}}\hat{\mathbf{i}}^T & \rightarrow \\ \leftarrow & {}^{\mathcal{A}}\hat{\mathbf{j}}^T & \rightarrow \\ \leftarrow & {}^{\mathcal{A}}\hat{\mathbf{k}}^T & \rightarrow \end{pmatrix} \tag{54}$$

The components of $\hat{\mathbf{i}}$ and $\hat{\mathbf{j}}$ drop out, so,

$$\mathbf{Q}_k(\theta) = \begin{pmatrix} k_x k_x(1-c\theta)+c\theta & k_x k_y(1-c\theta)-k_z s\theta & k_x k_z(1-c\theta)+k_y s\theta \\ k_x k_y(1-c\theta)+k_z s\theta & k_y k_y(1-c\theta)+c\theta & k_y k_z(1-c\theta)-k_x s\theta \\ k_x k_z(1-c\theta)-k_y s\theta & k_y k_z(1-c\theta)+k_x s\theta & k_z k_z(1-c\theta)+c\theta \end{pmatrix} \tag{55}$$

Conversely, the axis-angle parameters, expressed in terms of, $\mathbf{Q}$, are

$$\theta = \cos^{-1}\left(\frac{Q_{11}+Q_{22}+Q_{33}-1}{2}\right) \tag{56}$$

$$k_x = \frac{Q_{32}-Q_{23}}{2\sin\theta} \tag{57}$$

$$k_y = \frac{Q_{13}-Q_{31}}{2\sin\theta} \tag{58}$$

$$k_z = \frac{Q_{21}-Q_{12}}{2\sin\theta} \tag{59}$$

A.3 Euler Sets

The Euler angle scheme specifies a sequence of relative frame rotations about the principal axes. For example, an *xyz* sequence specifies a rotation of α about the x axis of the base frame, $\mathcal{A}$. Next a rotation of β is specified about the y axis of the intermediate frame associated with the completion of the first rotation, $\mathcal{A}'$. Finally a rotation of γ is specified about the z axis of the intermediate frame associated with the completion of the second rotation, $\mathcal{A}''$. *Figure A.3* depicts this sequence.

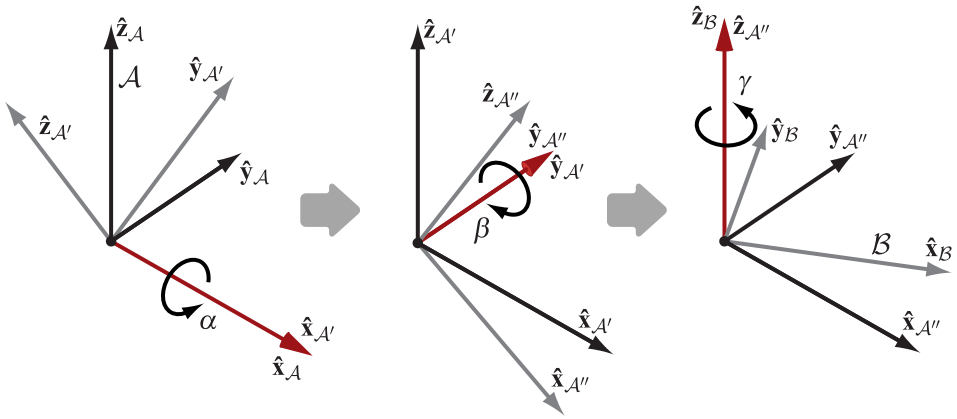

Figure A.3. An *xyz* Euler angle sequence specifies a rotation of α about the x axis of $\mathcal{A}$. Next a rotation of β is specified about the y axis of $\mathcal{A}'$. Finally, a rotation of γ is specified about the z axis of $\mathcal{A}''$.

The rotation matrix, ${}^{\mathcal{A}}_{\mathcal{B}}\mathbf{Q}$, associated with this rotation sequence is given by,

$${}^{\mathcal{A}}_{\mathcal{B}}\mathbf{Q}(\alpha,\beta,\gamma) = {}^{\mathcal{A}}_{\mathcal{A}'}\mathbf{Q}(\alpha)\,{}^{\mathcal{A}'}_{\mathcal{A}''}\mathbf{Q}(\beta)\,{}^{\mathcal{A}''}_{\mathcal{B}}\mathbf{Q}(\gamma) \tag{60}$$

Since all of these intermittent rotations are about principal axes we have,

$${}^{\mathcal{A}}_{\mathcal{B}}\mathbf{Q}(\alpha,\beta,\gamma) = \mathbf{Q}_{xyz}(\alpha,\beta,\gamma) = \mathbf{Q}_x(\alpha)\mathbf{Q}_y(\beta)\mathbf{Q}_z(\gamma) = \begin{pmatrix} 1 & 0 & 0 \\ 0 & \cos\alpha & -\sin\alpha \\ 0 & \sin\alpha & \cos\alpha \end{pmatrix} \begin{pmatrix} \cos\beta & 0 & \sin\beta \\ 0 & 1 & 0 \\ -\sin\beta & 0 & \cos\beta \end{pmatrix} \begin{pmatrix} \cos\gamma & -\sin\gamma & 0 \\ \sin\gamma & \cos\gamma & 0 \\ 0 & 0 & 1 \end{pmatrix} \tag{61}$$

So,

$$ {}^{\mathcal{A}}_{\mathcal{B}}\mathbf{Q}(\alpha,\beta,\gamma) = \begin{pmatrix} c\beta c\gamma & -c\beta s\gamma & s\beta \\ s\alpha s\beta c\gamma + c\alpha s\gamma & -s\alpha s\beta s\gamma + c\alpha c\gamma & -s\alpha c\beta \\ -c\alpha s\beta c\gamma + s\alpha s\gamma & c\alpha s\beta s\gamma + s\alpha c\gamma & c\alpha c\beta \end{pmatrix} \tag{62} $$

In general, for an arbitrary sequence *abc*, where,

$$ a = x, y, \text{ or } z \tag{63} $$
$$ b = x, y, \text{ or } z \tag{64} $$
$$ c = x, y, \text{ or } z \tag{65} $$
$$ a \neq b,\ b \neq c \tag{66} $$

we have,

$$ \mathbf{Q}_{abc}(\alpha,\beta,\gamma) = \mathbf{Q}_a(\alpha)\mathbf{Q}_b(\beta)\mathbf{Q}_c(\gamma) \tag{67} $$

The inverse problem of determining the Euler angles in terms of the rotation matrix can also be solved. For the *xyz* sequence addressed above we have the following solution:

If $\cos\beta \neq 0$, $(\beta \neq \pm\pi/2)$,

$$ \beta = \text{Atan2}(Q_{13}, \sqrt{Q_{11}^2 + Q_{12}^2}) \tag{68} $$
$$ \alpha = \text{Atan2}(-Q_{23}/c\beta, Q_{33}/c\beta) \tag{69} $$
$$ \gamma = \text{Atan2}(-Q_{12}/c\beta, Q_{11}/c\beta) \tag{70} $$

If $\beta = \pm\pi/2$,

$$ \alpha = 0 \tag{71} $$
$$ \gamma = \text{Atan2}(Q_{21}, Q_{22}) \tag{72} $$

For a *xzx* Euler sequence we have,

$$ \mathbf{Q}_{xzx}(\alpha,\beta,\gamma) = \begin{pmatrix} c\beta & -s\beta c\gamma & s\beta s\gamma \\ c\alpha s\beta & c\alpha c\beta c\gamma - s\alpha s\gamma & -c\alpha c\beta s\gamma - s\alpha c\gamma \\ s\alpha s\beta & s\alpha c\beta c\gamma + c\alpha s\gamma & -s\alpha c\beta s\gamma + c\alpha c\gamma \end{pmatrix} \tag{73} $$

and the solution to the inverse problem is,

If $\sin\beta \neq 0$, $(\beta \neq 0, \pi)$,

$$ \beta = \text{Atan2}(\sqrt{Q_{21}^2 + Q_{31}^2}, Q_{11}) \tag{74} $$
$$ \alpha = \text{Atan2}(Q_{31}/s\beta, Q_{21}/s\beta) \tag{75} $$
$$ \gamma = \text{Atan2}(Q_{13}/s\beta, -Q_{12}/s\beta) \tag{76} $$

If $\beta = 0$,

$$ \alpha = 0 \tag{77} $$
$$ \gamma = \text{Atan2}(Q_{32}, Q_{22}) \tag{78} $$

If $\beta = \pi$,

$$ \alpha = 0 \tag{79} $$
$$ \gamma = \text{Atan2}(Q_{32}, -Q_{22}) \tag{80} $$

A.4 Quaternions

A quaternion is a hyper-complex number which is the 4-dimensional analog to the 2-dimensional complex number $z = a + \mathbf{i}b$. The 4-dimensional space of quaternions, denoted by $\mathbb{H}$, is spanned by four orthogonal axes. These include the real axis and three principal imaginaries, $\mathbf{i}, \mathbf{j},$ and $\mathbf{k}$.

$$h = h_0 + h_1\mathbf{i} + h_2\mathbf{j} + h_3\mathbf{k} \tag{81}$$

This can also be thought of as a scalar part, h_0, and a vector part, $\mathbf{h}$.

$$h = h_0 + \mathbf{h} \tag{82}$$

Quaternion algebra is non-commutative with respect to multiplication. As such, the following laws apply:

$$\begin{aligned} \mathbf{i}^2 = \mathbf{j}^2 = \mathbf{k}^2 = \mathbf{ijk} = -1 \\ \mathbf{ij} = \mathbf{k} = -\mathbf{ji} \\ \mathbf{jk} = \mathbf{i} = -\mathbf{kj} \\ \mathbf{ki} = \mathbf{j} = -\mathbf{ik} \end{aligned} \tag{83}$$

Multiplication of two quaternions can most easily be represented using the operations of vector cross product and dot product. Given a quaternion, s, as the product of quaternions, g and h, we have,

$$s = gh = s_0 + \mathbf{s} \tag{84}$$

$$s = g_0h_0 - \mathbf{g}\cdot\mathbf{h} + g_0\mathbf{h} + h_0\mathbf{g} + \mathbf{g}\times\mathbf{h} \tag{85}$$

Grouping the scalar and vector parts separately, we have,

$$s_0 = g_0h_0 - \mathbf{g}\cdot\mathbf{h} \tag{86}$$

$$\mathbf{s} = g_0\mathbf{h} + h_0\mathbf{g} + \mathbf{g}\times\mathbf{h} \tag{87}$$

It is stressed that quaternions are not vectors, but rather hyper complex numbers. Nevertheless the components of the imaginary part of a quaternion can be used in traditional vector operations to compute quaternion products per the formula above. An equivalent algorithm exists for representing multiplication of two quaternions using matrix operations.

$$\begin{pmatrix} s_0 & s_1 & s_2 & s_3 \end{pmatrix} = \begin{pmatrix} g_0 & g_1 & g_2 & g_3 \end{pmatrix} \mathbf{H} \tag{88}$$

where $\mathbf{H}$ is a anti-symmetric matrix defined in terms of h as,

$$\mathbf{H} = \begin{pmatrix} h_0 & h_1 & h_2 & h_3 \\ -h_1 & h_0 & -h_3 & h_2 \\ -h_2 & h_3 & h_0 & -h_1 \\ -h_3 & -h_2 & h_1 & h_0 \end{pmatrix} \tag{89}$$

It is also convenient to represent a quaternion using complex matrices. First we define the following matrices in $\mathbb{C}^{2\times2}$,

$$\mathbf{1} = \begin{pmatrix} 1 & 0 \\ 0 & 1 \end{pmatrix}, \quad \mathbf{I} = \begin{pmatrix} \mathbf{i} & 0 \\ 0 & -\mathbf{i} \end{pmatrix}, \quad \mathbf{J} = \begin{pmatrix} 0 & 1 \\ -1 & 0 \end{pmatrix}, \quad \mathbf{K} = \begin{pmatrix} 0 & \mathbf{i} \\ \mathbf{i} & 0 \end{pmatrix} \tag{90}$$

The principal imaginaries, $\mathbf{I}, \mathbf{J}$, and $\mathbf{K}$ adhere to the same laws stated earlier, namely,

$$\begin{gathered}\mathbf{I}^2 = \mathbf{J}^2 = \mathbf{K}^2 = \mathbf{IJK} = -\mathbf{1} \\ \mathbf{IJ} = \mathbf{K} = -\mathbf{JI} \\ \mathbf{JK} = \mathbf{I} = -\mathbf{KJ} \\ \mathbf{KI} = \mathbf{J} = -\mathbf{IK}\end{gathered} \tag{91}$$

The quaternion is then,

$$\mathbf{H} = h_0 + h_1\mathbf{I} + h_2\mathbf{J} + h_3\mathbf{K} = \begin{pmatrix} h_0 + \mathbf{i}h_1 & h_2 + \mathbf{i}h_3 \\ -h_2 + \mathbf{i}h_3 & h_0 - \mathbf{i}h_1 \end{pmatrix} \tag{92}$$

While this is a useful representation of quaternions we will use the conventional representation throughout the remainder of this document, namely, $h = h_0 + h_1\mathbf{i} + h_2\mathbf{j} + h_3\mathbf{k}$. We can define the inverse of a quaternion, h^{-1}, as satisfying,

$$hh^{-1} = h^{-1}h = 1 + 0\mathbf{i} + 0\mathbf{j} + 0\mathbf{k}0 = 1 \tag{93}$$

Noting that the product of a quaternion and its conjugate, $\bar{h}$, is given by,

$$\begin{aligned} h\bar{h} &= (h_0 + h_1\mathbf{i} + h_2\mathbf{j} + h_3\mathbf{k})(h_0 - h_1\mathbf{i} - h_2\mathbf{j} - h_3\mathbf{k}) \\ &= h_0h_0 - \mathbf{h}\cdot\mathbf{h} + h_0\mathbf{h} + h_0\mathbf{h} + \mathbf{h}\times\mathbf{h} \\ &= h_0h_0 + h_1h_1 + h_2h_2 + h_3h_3 \\ &= \|h\|^2 \end{aligned} \tag{94}$$

we have,

$$h^{-1} = \frac{\bar{h}}{\|h\|^2} \tag{95}$$

A unit quaternion $\{h \,|\, \|h\| = 1\}$ is a point on a unit hypersphere, $\mathbb{S}^3 \subset \mathbb{H}$, where $h_0^2 + h_1^2 + h_2^2 + h_3^2 = 1$. Unit quaternions are efficient at encapsulating spatial rotation. There is a direct relationship between the elements of a unit quaternion and the axis-angle parameters. For any unit quaternion, $h \in \mathbb{S}^3$, we have,

$$h = \cos\frac{\theta}{2} + k_x\sin\frac{\theta}{2}\mathbf{i} + k_y\sin\frac{\theta}{2}\mathbf{j} + k_z\sin\frac{\theta}{2}\mathbf{k} = \cos\frac{\theta}{2} + \mathbf{u}\sin\frac{\theta}{2} \tag{96}$$

where,

$$\mathbf{u} = k_x\mathbf{i} + k_y\mathbf{j} + k_z\mathbf{k} \tag{97}$$

In shorthand we have,

$$h = e^{\frac{\theta}{2}\mathbf{u}} \text{ and } h^{-1} = \bar{h} = e^{-\frac{\theta}{2}\mathbf{u}} \tag{98}$$

The individual elements of a unit quaternion are also referred to as Euler parameters, $\varepsilon_1, \varepsilon_2, \varepsilon_3$, where,

$$\begin{gathered}\varepsilon_1 \triangleq h_1, \varepsilon_2 \triangleq h_2, \varepsilon_3 \triangleq h_3, \varepsilon_4 \triangleq h_0 \\ \varepsilon_1 = k_x\sin\frac{\theta}{2}, \varepsilon_2 = k_y\sin\frac{\theta}{2}, \varepsilon_3 = k_z\sin\frac{\theta}{2}, \varepsilon_1 = \cos\frac{\theta}{2}\end{gathered} \tag{99}$$

Rotational transformation can be accommodated with unit quaternions using a double product. To rotate a vector $\mathbf{v} \in \mathbb{R}^3$ about the $\mathbf{u}$ axis by an angle of θ we perform the following,

$$h\mathbf{v}h^{-1} = h\mathbf{v}\bar{h} = e^{\frac{\theta}{2}\mathbf{u}}\mathbf{v}e^{-\frac{\theta}{2}\mathbf{u}} \tag{100}$$

In this case the vector, **v**, is represented as a pure quaternion (real part equal to 0).

$$\mathbf{v} = v_1\mathbf{i} + v_2\mathbf{j} + v_3\mathbf{k} \tag{101}$$

In terms of frame transformations we have,

$${}^{\mathcal{A}}\mathbf{v} = {}^{\mathcal{A}}_{\mathcal{B}}h\,{}^{\mathcal{B}}\mathbf{v}\,{}^{\mathcal{B}}_{\mathcal{A}}h = {}^{\mathcal{A}}_{\mathcal{B}}h\,{}^{\mathcal{B}}\mathbf{v}\,{}^{\mathcal{A}}_{\mathcal{B}}\bar{h} \tag{102}$$

where,

$${}^{\mathcal{A}}_{\mathcal{B}}\bar{h} = {}^{\mathcal{A}}_{\mathcal{B}}h = {}^{\mathcal{B}}_{\mathcal{A}}h \tag{103}$$

Additionally, multiple rotations can be concatenated using multiplication, for example,

$${}^{\mathcal{A}}_{\mathcal{C}}h = {}^{\mathcal{A}}_{\mathcal{B}}h\,{}^{\mathcal{B}}_{\mathcal{C}}h \tag{104}$$

It is useful to relate the unit quaternion to the other representations of orientation. For axis-angle parameters we have:

$$\begin{array}{c} h_0 = \cos\frac{\theta}{2} \\ h_1 = k_x \sin\frac{\theta}{2} \\ h_2 = k_y \sin\frac{\theta}{2} \\ h_3 = k_z \sin\frac{\theta}{2} \end{array} \quad \text{and} \quad \begin{array}{c} \theta = 2\cos^{-1} h_0 \\ k_x = \frac{h_1}{\sqrt{1-h_0 h_0}} \\ k_y = \frac{h_2}{\sqrt{1-h_0 h_0}} \\ k_z = \frac{h_3}{\sqrt{1-h_0 h_0}} \end{array} \tag{105}$$

Relating a rotation matrix and unit quaternion we have,

$$\mathbf{Q}(h) = \begin{pmatrix} 2(h_0h_0 + h_1h_1) - 1 & 2(h_1h_2 - h_0h_3) & 2(h_1h_3 + h_0h_2) \\ 2(h_1h_2 + h_0h_3) & 2(h_0h_0 + h_2h_2) - 1 & 2(h_2h_3 - h_0h_1) \\ 2(h_1h_3 - h_0h_2) & 2(h_2h_3 + h_0h_1) & 2(h_0h_0 + h_3h_3) - 1 \end{pmatrix} \tag{106}$$

and,

$$h_0 = \frac{1}{2}\sqrt{1 + Q_{11} + Q_{22} + Q_{33}} \tag{107}$$

$$h_1 = \frac{Q_{32} - Q_{23}}{4h_0} \tag{108}$$

$$h_2 = \frac{Q_{13} - Q_{31}}{4h_0} \tag{109}$$

$$h_3 = \frac{Q_{21} - Q_{12}}{4h_0} \tag{110}$$

A.5 Calculus of Rotations

It will be useful to examine the rate of change for some of the orientation schemes that we have described. In particular, we can express the differential change of rotation matrices and unit quaternions as a differential spin about a fixed instantaneous axis. In doing this we arrive at the concept of angular velocity, thereby relating the derivative of an orientation operator to angular velocity. A relationship between angle-set derivatives and angular velocity can also be derived.

A.5.1 Derivative of the Rotation Matrix

We will now define the derivative of a rotation operator. Let us begin with the rotation matrix.

$$\dot{\mathbf{Q}} = \frac{d\mathbf{Q}}{dt} = \lim_{\Delta t \to 0} \frac{\mathbf{Q}(t+\Delta t) - \mathbf{Q}(t)}{\Delta t} \tag{111}$$

It will be convenient to express the time rate of change of a rotation operator in terms of an instantaneous spin rate and axis. This will entail applying a differential spin, $\Delta\theta$, about a fixed instantaneous axis. *Figure A.4* depicts this infinitesimal rotation.

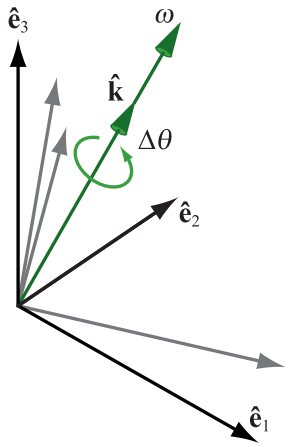

Figure A.4. Instantaneous spin about an axis. The incremental spin, $\Delta\theta$, about an axis, $\hat{\mathbf{k}}$, can be related to the angular velocity, ω.

Noting that,

$$\mathbf{Q}(t+\Delta t) = \mathbf{Q}_k(\Delta\theta)\mathbf{Q}(t) \tag{112}$$

the derivative can then be expressed as,

$$\dot{\mathbf{Q}} = \lim_{\Delta t \to 0} \frac{\mathbf{Q}_k(\Delta\theta)\mathbf{Q}(t) - \mathbf{Q}(t)}{\Delta t} = \left(\lim_{\Delta t \to 0} \frac{\mathbf{Q}_k(\Delta\theta) - \mathbf{1}}{\Delta t} \right) \mathbf{Q}(t) \tag{113}$$

where,

$$\mathbf{Q}_k(\Delta\theta) = \begin{pmatrix} k_x k_x(1-c\Delta\theta) + c\Delta\theta & k_x k_y(1-c\Delta\theta) - k_z s\Delta\theta & k_x k_z(1-c\Delta\theta) + k_y s\Delta\theta \\ k_x k_y(1-c\Delta\theta) + k_z s\Delta\theta & k_y k_y(1-c\Delta\theta) + c\Delta\theta & k_y k_z(1-c\Delta\theta) - k_x s\Delta\theta \\ k_x k_z(1-c\Delta\theta) - k_y s\Delta\theta & k_y k_z(1-c\Delta\theta) + k_x s\Delta\theta & k_z k_z(1-c\Delta\theta) + c\Delta\theta \end{pmatrix} \tag{114}$$

Noting small angle (infinitesimal in this case) properties,

$$\mathbf{Q}_k(\Delta\theta) = \begin{pmatrix} 1 & -k_z\Delta\theta & k_y\Delta\theta \\ k_z\Delta\theta & 1 & -k_x\Delta\theta \\ -k_y\Delta\theta & k_x\Delta\theta & 1 \end{pmatrix} \tag{115}$$

We then have,

$$\dot{\mathbf{Q}} = \begin{pmatrix} 0 & -k_z\dot{\theta} & k_y\dot{\theta} \\ k_z\dot{\theta} & 0 & -k_x\dot{\theta} \\ -k_y\dot{\theta} & k_x\dot{\theta} & 0 \end{pmatrix} \mathbf{Q}(t) = \begin{pmatrix} 0 & -\omega_z & \omega_y \\ \omega_z & 0 & -\omega_x \\ -\omega_y & \omega_x & 0 \end{pmatrix} \mathbf{Q}(t) \tag{116}$$

Defining the anti-symmetric angular velocity matrix, Ω, as,

$$\Omega = \begin{pmatrix} 0 & -\omega_z & \omega_y \\ \omega_z & 0 & -\omega_x \\ -\omega_y & \omega_x & 0 \end{pmatrix} \tag{117}$$

We have,

$$\dot{\mathbf{Q}} = \Omega\mathbf{Q} = \begin{pmatrix} 0 & -\omega_z & \omega_y \\ \omega_z & 0 & -\omega_x \\ -\omega_y & \omega_x & 0 \end{pmatrix} \mathbf{Q} \tag{118}$$

The matrix Ω is actually a rank two tensor and can thus be represented as the following dyadic,

$$\Omega = \Omega_{ij}\hat{\mathbf{e}}_i \otimes \hat{\mathbf{e}}_j = \omega_z(\hat{\mathbf{e}}_2 \otimes \hat{\mathbf{e}}_1 - \hat{\mathbf{e}}_1 \otimes \hat{\mathbf{e}}_2) + \omega_y(\hat{\mathbf{e}}_1 \otimes \hat{\mathbf{e}}_3 - \hat{\mathbf{e}}_3 \otimes \hat{\mathbf{e}}_1) + \omega_x(\hat{\mathbf{e}}_3 \otimes \hat{\mathbf{e}}_2 - \hat{\mathbf{e}}_2 \otimes \hat{\mathbf{e}}_3) \tag{119}$$

The above has been formulated with the spin axis represented in the base frame. Any frame representation can be used.

$$\overset{\mathcal{A}}{\mathcal{B}}\dot{\mathbf{Q}} = {}^{\mathcal{A}}\Omega \overset{\mathcal{A}}{\mathcal{B}}\mathbf{Q} = \overset{\mathcal{A}}{\mathcal{B}}\mathbf{Q}\,{}^{\mathcal{B}}\Omega \tag{120}$$

Frame transformations for the angular velocity matrix can be accommodated with the double product.

$${}^{\mathcal{A}}\Omega = \overset{\mathcal{A}}{\mathcal{B}}\mathbf{Q}\,{}^{\mathcal{B}}\Omega\,\overset{\mathcal{B}}{\mathcal{A}}\mathbf{Q} \tag{121}$$

A.5.2 Derivative of the Unit Quaternion

Defining the derivative of a unit quaternion, we have,

$$\dot{h} = \frac{dh}{dt} = \lim_{\Delta t \to 0} \frac{h(t+\Delta t) - h(t)}{\Delta t} \tag{122}$$

Applying a differential spin, $\Delta\theta$, about a fixed instantaneous axis (see *Figure A.4*) gives us,

$$h(t+\Delta t) = h_k(\Delta\theta)h(t) \tag{123}$$

The derivative can then be expressed as,

$$\dot{h} = \lim_{\Delta t \to 0} \frac{h_k(\Delta\theta)h(t) - h(t)}{\Delta t} = \left(\lim_{\Delta t \to 0} \frac{h_k(\Delta\theta) - 1}{\Delta t} \right) h(t) \tag{124}$$

where,

$$h_k(\Delta\theta) = \cos\frac{\Delta\theta}{2} + k_x \sin\frac{\Delta\theta}{2}\mathbf{i} + k_y \sin\frac{\Delta\theta}{2}\mathbf{j} + k_z \sin\frac{\Delta\theta}{2}\mathbf{k} \tag{125}$$

Noting small angle (infinitesimal in this case) properties,

$$h_k(\Delta\theta) = 1 + k_x\frac{\Delta\theta}{2}\mathbf{i} + k_y\frac{\Delta\theta}{2}\mathbf{j} + k_z\frac{\Delta\theta}{2}\mathbf{k} \tag{126}$$

We then have,

$$\dot{h} = \left(0 + k_x \frac{\dot{\theta}}{2}\mathbf{i} + k_y \frac{\dot{\theta}}{2}\mathbf{j} + k_z \frac{\dot{\theta}}{2}\mathbf{k}\right) h(t) = \left(0 + \frac{\omega_x}{2}\mathbf{i} + \frac{\omega_y}{2}\mathbf{j} + \frac{\omega_z}{2}\mathbf{k}\right) h(t) \tag{127}$$

where ω is the angular velocity represented as a quaternion.

$$\omega = 0 + \omega_x\mathbf{i} + \omega_y\mathbf{j} + \omega_z\mathbf{k} \tag{128}$$

So, we have,

$$\dot{h} = \frac{1}{2}\omega h \tag{129}$$

As in the case of the derivative of the rotation matrix, the above has been formulated with the spin axis represented in the base frame. Any frame representation can be used.

$${}^{\mathcal{A}}_{\mathcal{B}}\dot{h} = \frac{1}{2}{}^{\mathcal{A}}\omega\, {}^{\mathcal{A}}_{\mathcal{B}}h = \frac{1}{2}{}^{\mathcal{A}}_{\mathcal{B}}h\, {}^{\mathcal{B}}\omega \tag{130}$$

Frame transformations for the angular velocity quaternion can be accommodated with the familiar double product.

$${}^{\mathcal{A}}\omega = {}^{\mathcal{A}}_{\mathcal{B}}h\, {}^{\mathcal{B}}\omega\, {}^{\mathcal{B}}_{\mathcal{A}}h \tag{131}$$

Table A.1 lists various dualities between the rotation matrix and the unit quaternion.

Property	Rotation Matrix	Quaternion
Identity	$\mathbf{1} = \begin{pmatrix} 1 & 0 & 0 \\ 0 & 1 & 0 \\ 0 & 0 & 1 \end{pmatrix}$	$1 = 1 + 0\mathbf{i} + 0\mathbf{j} + 0\mathbf{k}$
Inverse	$\mathbf{Q}^{-1} = \mathbf{Q}^T$	$h^{-1} = \bar{h}$
Derivative	$\dot{\mathbf{Q}} = \Omega\mathbf{Q}$	$\dot{h} = \frac{1}{2}\omega h$
Angular Velocity	$\Omega = \begin{pmatrix} 0 & -\omega_z & \omega_y \\ \omega_z & 0 & -\omega_x \\ -\omega_y & \omega_x & 0 \end{pmatrix}$	$\omega = 0 + \omega_x\mathbf{i} + \omega_y\mathbf{j} + \omega_z\mathbf{k}$
Transformation	${}^{\mathcal{A}}\Omega = {}^{\mathcal{A}}_{\mathcal{B}}\mathbf{Q}\, {}^{\mathcal{B}}\Omega\, {}^{\mathcal{B}}_{\mathcal{A}}\mathbf{Q}$	${}^{\mathcal{A}}\omega = {}^{\mathcal{A}}_{\mathcal{B}}h\, {}^{\mathcal{B}}\omega\, {}^{\mathcal{B}}_{\mathcal{A}}h$

Table A.1. Duality between Rotation Matrix and Unit Quaternion

A.5.3 Derivative of the Angle Sets

We have thus far related rotation matrices and quaternions to angular velocity. We can also relate rates of change of Euler and fixed angles (angle sets) to angular velocity. The rate vector of a given angle set is,

$$\dot{\phi} = \begin{pmatrix} \dot{\alpha} \\ \dot{\beta} \\ \dot{\gamma} \end{pmatrix} \tag{132}$$

Noting the relationship between a rotation matrix and angular velocity,

$$\Omega = \begin{pmatrix} 0 & -\omega_z & \omega_y \\ \omega_z & 0 & -\omega_x \\ -\omega_y & \omega_x & 0 \end{pmatrix} \dot{\mathbf{Q}}\mathbf{Q}^T \tag{133}$$

we can determine the following,

$$\omega = \begin{pmatrix} \omega_x \\ \omega_y \\ \omega_z \end{pmatrix} = \begin{pmatrix} \dot{Q}_{31}Q_{21} + \dot{Q}_{32}Q_{22} + \dot{Q}_{33}Q_{23} \\ \dot{Q}_{11}Q_{31} + \dot{Q}_{12}Q_{32} + \dot{Q}_{13}Q_{33} \\ \dot{Q}_{21}Q_{11} + \dot{Q}_{22}Q_{12} + \dot{Q}_{23}Q_{13} \end{pmatrix} \tag{134}$$

We note that,

$$\dot{Q}_{ij} = \frac{\partial Q_{ij}}{\partial \phi}\dot{\phi} \tag{135}$$

So angular velocity is related to the angle set rate vector by the following relationship,

$$\omega = \begin{pmatrix} \omega_x \\ \omega_y \\ \omega_z \end{pmatrix} = \begin{pmatrix} \frac{\partial Q_{31}}{\partial \phi}Q_{21} + \frac{\partial Q_{32}}{\partial \phi}Q_{22} + \frac{\partial Q_{33}}{\partial \phi}Q_{23} \\ \frac{\partial Q_{11}}{\partial \phi}Q_{31} + \frac{\partial Q_{12}}{\partial \phi}Q_{32} + \frac{\partial Q_{13}}{\partial \phi}Q_{33} \\ \frac{\partial Q_{21}}{\partial \phi}Q_{11} + \frac{\partial Q_{22}}{\partial \phi}Q_{12} + \frac{\partial Q_{23}}{\partial \phi}Q_{13} \end{pmatrix} \dot{\phi} = \mathbf{E}(\phi)\dot{\phi} \tag{136}$$

where $\mathbf{E}(\phi)$ is the Jacobian between angular velocity and angle set rates.

DISTRIBUTION:

1	MS	9155	Robert Clay, 8953
2	MS	9159	Vincent De Sapio, 8953
2	MS	9152	Jeffrey Jortner, 8953
2	MS	9018	Central Technical Files, 8945-1
2	MS	0899	Technical Library, 4536

Sandia National Laboratories